

**Characterization of Nonpoint Source Microbial Contamination in an
Urbanizing Watershed Serving as a Municipal Water Supply**

By Jakob Rowny

A thesis submitted to the faculty of the University of North Carolina at Chapel Hill in partial fulfillment of the requirements for the degree of Master of Science in the Department of Environmental Sciences and Engineering

Chapel Hill

2011

Approved by:
Dr. Jill R. Stewart
Dr. Gregory W. Characklis
Dr. Rose M. Cory

© 2011

Jakob Rowny

ALL RIGHTS RESERVED

Abstract

Jakob Rowny: Characterization of Nonpoint Source Microbial Contamination in an Urbanizing Watershed Serving as a Municipal Water Supply
(Under the direction of Dr. Jill R. Stewart)

Inland watersheds in the Southeastern United States are transitioning from agriculture and forested land uses to urban and exurban uses at a rate greater than the national average. This study sampled creeks representing a variety of land use factors in the rapidly urbanizing Jordan Lake watershed. Samples were collected bimonthly under dry-weather conditions and four times during each of three storm events and assessed for traditional microbial indicators of water quality. Fecal indicator bacteria (FIB) concentrations were generally higher in more developed watersheds. FIB concentrations were significantly greater during storm events than during dry-weather conditions, although concentrations demonstrated both intra and inter-storm variability. These results indicate that the magnitude of microbial contamination is influenced by intensity of watershed development, streamflow and antecedent precipitation. Dry-weather FIB loads showed considerable seasonal variation, but the average storm event delivered contaminant loads equivalent to months of dry-weather loading. Analysis of intra-storm loading patterns provided little evidence to support “first-flush” loading of either FIB. These findings could potentially inform watershed management and public health decisions related to the urbanization of watersheds serving as municipal sources of drinking water.

Acknowledgements

This research was supported in part by the NC Water Resources Research Institute (NC WRRRI) project #70252. Many individuals provided assistance with lab and field work: Stephanie Schumaker, Kelli Paice, Jennifer Shields, Angela Wang, Emylee Prevette, Robert Albury, Kevin Meyers, Sarah Hatcher, Maya Nadimpalli, Hunter Storey, Jonathan Crocker and Jordan Kern. Thanks also to Curtis Stumpf for information on loading analysis methods; Stephanie Wendell for watershed delineation methods and Dr. Lawrence Band for providing guidance on site selection and GIS data. I would also like to thank my committee members: Dr. Jill Stewart, Dr. Greg Characklis and Dr. Rose Cory.

Table of Contents

List of Tables	vii
List of Figures	ix
Introduction	1
Study Area.....	9
Objectives	10
Materials and Methods	10
Site Selection.....	10
Impervious Surfaces and Land Use	11
Watershed Area	11
Precipitation and Stream Flow.....	12
Sampling Design	14
Dry-weather Sampling	14
Storm Event Sampling.....	15
Detection of Indicator Species	16
Statistical Methods.....	16
Results and Discussion	17
Physical and Chemical Parameters	17
Loading Analysis and Characterization	18

Pollutant Mass to Volume Curves	21
FIB Concentration Patterns.....	24
Dry-Weather and Storm Event FIB Concentrations.....	25
Precipitation, Streamflow and Water Temperature	27
Land cover, Impervious Surfaces and FIB Concentrations	30
Land Cover Change, 1999-2005	30
Correlations of Land Cover, Impervious Surfaces and FIB Concentrations	31
Correlations of Land Cover, Impervious Surfaces and Total Loads Normalized for Watershed Area	32
Development Intensity and Watershed Area	33
3-factor ANOVA.....	35
Conclusions	36
Appendix A: Supplementary Tables and Figures.....	38
References.....	51

List of Tables

Table 1: Study sites	13
Table 2: Storm event precipitation statistics and storm event FIB loading, all creeks combined	18
Table 3: Seasonal dry-weather FIB loading, all creeks combined	19
Table 4: Average dry-weather (DW) and average storm event FIB loads for all creeks and equivalent days of dry-weather necessary to equal event loading of both FC and EC.....	20
Table 5: Dry-Weather (DW) and storm event mean concentrations (EMC) for all creeks and one way ANOVA test results.....	20
Table 6: Range and average of FC and EC mass loading after initial 30% volume storm runoff for individual creeks and all creeks combined.....	23
Table 7: Summary statistics of FIB concentrations during dry-weather and storm events, all creeks combined.....	26
Table 8: Summary statistics of dry-weather and storm event FIB concentrations (CFU/100 ml), all creeks and all storms combined.....	27
Table 9: Spearman’s rank correlations (R^2) of all creeks combined and individual creek sites for measures of streamflow (m^3/sec) and antecedent precipitation (mm) vs. EC concentrations ($\log_{10}(x + 1)$ CFU/100 ml).....	28
Table 10: Spearman’s rank correlations (R^2) of all creeks combined and individual creek sites for measures of streamflow (m^3/sec) and antecedent precipitation vs. FC concentrations ($\log_{10}(x + 1)$ CFU/100 ml).....	29
Table 11: Land cover and imperviousness of individual creek watersheds in Oct. 1999, Oct. 2005 and percent change.....	31
Table 12: Spearman’s rank-order correlations (R^2) of log-transformed FIB concentrations, land cover measures and impervious surface (IS) coverage during dry-weather (DW) and storm events.....	32
Table 13: Spearman’s rank-order correlations of log-transformed watershed area normalized FIB total loads, land cover measures and impervious surface (IS) coverage during dry-weather (DW) and storm events.	33
Table 14: Summary statistics of FIB concentrations (CFU/100 ml) by development intensity class and sample type	33

Table 15: Summary statistics of FIB concentrations (CFU/100 ml) by watershed area and sample type.....	34
Table 16: Results of 3-factor ANOVAs and pair-wise comparisons performed on log-transformed FIB concentrations.....	36
Table 17: Storm event loading, Morgan Creek at White Cross, NC (MCWC).....	39
Table 18: Storm event loading, Meeting of the Waters Creek (MWC).....	39
Table 19: Storm event loading, Morgan Creek at NC-1726 (MC1726).	40
Table 20: Storm event loading, New Hope Creek at Blands (NHCB).	40
Table 21: Storm event loading, Northeast Creek at Genlee (NECG).	40
Table 22: Storm event loading, Third Fork NHC at Woodcroft Parkway (TFWP).	40
Table 23: Storm event loading, Sandy Creek at Cornwallis Rd (SC).	41
Table 24: Summary of measured parameters during dry-weather (DW), storm events and combined, all creek sites.....	41

List of Figures

Figure 1: Study area showing sampling points and the New Hope Creek branch of Jordan Lake, N.C. (USA).	14
Figure 2: Average mass to volume (M/V) curves for (A) FC and (B) EC at each gauged creek site.	22
Figure 3: Correlation between log-transformed FC and EC concentrations during both dry-weather and storm events. *Pearson’s correlations significant at $p < 0.001$	25
Figure 4: Summary box plots of log- transformed FC (left) and EC (right) concentrations across all creeks and all storms.	26
Figure 5: Correlations of log-transformed FIB concentrations and water temperature. *Spearman’s rank correlations significant at $p < 0.001$	30
Figure 6: Tukey box plots divided by development intensity (DI) class and sample type: FC (left) and EC (right).	34
Figure 7: Tukey box plots divided by watershed area and sample type: FC (left) and EC (right).	35
Figure 8: Storm event 1 hydrographs at all gauged creeks.	38
Figure 9: Storm event 2 hydrographs at all gauged creeks.	38
Figure 10: Storm event 3 hydrographs at all gauged creeks.	39
Figure 11: Seasonal variation in daily dry-weather FIB load at all gauged creek sites and all creek sites combined.	41
Figure 12: Storm event loading patterns at all gauged creek sites and all creek sites combined.	42
Figure 13: Individual FC M/V curves, Morgan Creek at NC-54 West (MCWC).	43
Figure 14: Individual EC M/V curves, Morgan Creek at NC-54 West (MCWC).	43
Figure 15: Individual FC M/V curves, Meeting of the Water Creek (MWC).	44
Figure 16: Individual EC M/V curves, Meeting of the Water Creek (MWC).	44
Figure 17: Individual FC M/V curves, Morgan Creek at NC-1726 (MC1726).	45

Figure 18: Individual EC M/V curves, Morgan Creek at NC-1726 (MC1726).	45
Figure 19: Individual FC M/V curves, New Hope Creek at Blands (NHCB).	46
Figure 20: Individual EC M/V curves, New Hope Creek at Blands (NHCB).	46
Figure 21: Individual FC M/V curves, Northeast Creek at Genlee (NECG).	47
Figure 22: Individual EC M/V curves, Northeast Creek at Genlee (NECG).	47
Figure 23: Individual FC M/V curves, Third Fork NHC at Woodcroft Parkway (TFWB).	48
Figure 24: Individual EC M/V curves, Third Fork NHC at Woodcroft Parkway (TFWB).	48
Figure 25: Individual FC M/V curves, Sandy Creek at Cornwallis Rd (SC).	49
Figure 26: Individual EC M/V curves, Sandy Creek at Cornwallis Rd (SC).	49
Figure 27: Detail of “bridge buddy” sample collection device being readied for use.	50
Figure 28: A field technician prepares to collect a sample by lowering the device into the creek below.	50

Introduction

Nonpoint source (NPS) pollution is a leading cause of impaired surface waters in the United States of America. Precipitation events and associated storm water runoff deliver many types of contaminants to receiving surface waters, but sediment, nutrient and microbial agents are often a primary concern. Section 303 (d) of The Clean Water Act requires states, tribes and other authorities to assess and report the impairment of surface water. On a national scale, the greatest cause of reported 303 (d) impairment is pathogen contamination, as measured by various fecal indicator bacteria (FIB), accounting for 15.2 % of 70,753 listings, while nutrient contamination is the third leading cause (9.7%) and sediments (8.8%) rank fourth (USEPA, 2010). Although some surface water impairment may be caused by point sources, storm water has been indicated to significantly increase the contaminant loading of surface waters over baseline, dry weather conditions (Stumpf et al, 2010; Mallin et al, 2008; Krometis, 2007; Surbeck et al, 2006; Schueler 1994). The increase in NPS contaminant loading has been attributed to a variety of factors such as hydrology, geology, and climate as well as the intensity and type of watershed land uses.

Land use can be divided into two primary categories: rural and urban. Of the approximate land base of 9,300,000 km² in the United States, 97% is classified as rural and is used for a wide variety of purposes including agriculture (range, cropland, pasture and farmsteads), forest-use land, parks, wilderness, wildlife and other special uses, or is considered barren (USDA, 2005). The remaining 3% (approximately 243,000 km²) is classified as urban. Land use varies considerably by region, as do trends in the change of uses over time. For instance, in the Southeast 7.1% of 500,000

km² is urban and 12.0% is used as cropland, while in the Northern Plains only 0.5% of 410,000 km² is urban and 52.5% is cropland. The primary trends in land use change in the United States over the course of the last half century have been the conversion of lands used for agriculture and a rapid increase in urban and exurban development. On the national level between 1950 and 2000 cropland use decreased from 35% to 31% while urban and exurban areas increased from 1% to nearly 3% (USDA, 2005; Brown et al, 2005). This trend was especially pronounced in the Mid Atlantic and Southeast regions, where strong economic and demographic forces have driven population growth and the conversion of agricultural and forested lands to urban and exurban ones at a rate greater than the national average (Milesi, 2003). Furthermore, some estimates project this trend to continue, especially in the South and Southeast, where urban areas are expected to double between 1992 and 2020 (Wear and Greis, 2002).

NPS pollution resulting from agricultural land use, especially in watersheds intensively used as croplands and as livestock feeding areas is particularly well studied. Beginning in the late 1970's, as regulators achieved greater success in controlling point source pollution resulting from industrial and wastewater treatment plants, researchers began to shift towards the assessment of NPS pollution (Baker, 1992). Agriculture had been quickly identified as a major NPS and the earliest 303 (d) surface water reports clearly indicate the significance of the problem: agriculture accounted for 41% of reported NPS impacts to rivers, 23% of impacts to lakes and 7% percent of impacts to estuaries. In comparison, reports resulting from urban NPS pollution were much fewer, just 4%, 6% and 11% of the totals, while mining accounted for 8%, 7% and, 16% of reports, respectively (USEPA, 1990).

The primary constituents of NPS pollution from agricultural lands include sediments, nutrients, pesticides, salinity and microbial pathogens. Sedimentation of surface waters is most

commonly caused by poorly implemented soil conservation and erosion control and can negatively affect water quality, diminish dissolved oxygen, and change species composition by altering stream morphology (Karr and Dudley, 1981; Lenat, 1984). Although sedimentation remains a problem in agricultural watersheds, the impact of this constituent has been reduced by the development and implementation of best management practices (BMPs) such as buffer strips (Barling and Moore, 1994), sedimentation basins and other constructed wetlands (Hammer, 1992). Nutrients, particularly Phosphorous and Nitrogen are more persistent agricultural NPS pollutants. Nutrient NPS pollution is primarily the result of over application of chemical and manure fertilizers onto croplands, although livestock grazing has been shown to contribute to this problem as well (Edwards and Daniel 1992). Like agricultural sedimentation, nutrient NPS pollution is caused by erosion and runoff, but in addition has been shown to be mediated by sub-surface and surface movement of dissolved ions when soils reach and exceed maximum nutrient saturation (Sims et al, 1998; Nash, 2000). One consequence of nutrient NPS pollution is the Eutrophication of surface waters, which can result in phytoplanktonic blooms that have many adverse effects on surface waters and coastal ocean systems including anoxia, fish kills, change in species composition, loss of biodiversity and odor, taste and water treatment problems (Smith, 1998; Carpenter et al, 1998). Microbial NPS pollution is most common in agricultural watersheds where crops are fertilized with animal manure or by the direct input from livestock themselves (Carpenter et al, 1998). The later source has become more important with the escalating industrialization of livestock operations and the increasing use of manure lagoons where concentrated fecal waste can seep or overflow into surface waters, or are disposed of by being sprayed onto non-crop lands (Mallin and Cahoon, 2003).

NPS pollution resulting from urban land use has some similarities with agricultural NPS pollution. Both types of land use increase nutrient and microbial NPS pollution. However, pollutants common to agricultural watersheds such as sediments, pesticides and salinity are often less

important contaminants in urban watersheds. Another important difference is that the built watershed of the urban environment affects the timing, distribution, loading and constituent parts of contaminant runoff differently than the less intensively developed rural watershed. This is driven primarily by the greater impervious surface cover of urban areas. Impervious surfaces include roads, sidewalks, parking lots, rooftops, and other constructions that inhibit the infiltration of water into the ground. Impervious surfaces not only reduce the absorption of precipitation and increase the total volume of water runoff; they also contribute to the velocity, spatial pattern and timing of runoff and increase the concentration or total loading of NPS contaminants (Schueler, 1994).

Beginning in the 1990's, researchers began to recognize that measures of imperviousness (expressed as a percentage of total watershed area) could be used as a metric of ecological health and water quality both within and between different urban watersheds. A growing number of studies indicated a clear correlation between increasing imperviousness and stream channel instability and stream bank erosion (Booth and Jackson, 1997) that could lead to a variety of other changes such as increasing stream temperature (Galli, 1990), loss of aquatic habitat quality (Booth, 1991 as cited in Schueler, 1995), loss of stream diversity as measured by a variety of indicator species such as aquatic insects (Jones and Clark, 1987; Steedman, 1988) and fish (Booth, 1991; Limburg and Schmidt, 1990) as well as increasing NPS pollution (Mallin et al, 2000). Interestingly, despite the wide variety of metric or indicator used, the results indicate that abrupt levels of ecological degradation to streams begin to occur at relatively low levels of imperviousness, usually between 8-15% (often averaged to 10%), regardless of investigated indicator. Arnold and Gibbons (1996) suggested that there is also a higher threshold, at imperviousness levels above 30% where degradation reaches severe levels leading to precipitous declines in stream health that cannot be mitigated by traditional BMPs.

However, the generalization that watershed imperviousness could be used as a simple indicator of environmental or ecological health and water quality, and that there were clear thresholds that demarcated healthy and unhealthy watersheds quickly came under scrutiny. For instance, Booth and Jackson (1997) noted that most of the underlying research rarely described what method was used in the determination of imperviousness and did not distinguish between total impervious area (TIA) and effective impervious area (EIA). They defined TIA as the “intuitive” measure of imperviousness: the fraction of watershed covered by constructed, non-infiltrating surfaces such as concrete, asphalt and buildings. However, this characterization is incomplete and ignores two important hydrological factors. The first is that it does not include nominally “pervious” surfaces such as improperly rehabilitated or degraded urban areas, parklands, lawns and other surfaces that demonstrate lower permeability than completely undisturbed land. The second factor is that this definition of imperviousness includes impervious areas that contribute no additional runoff. An example of this is rooftop runoff that does not drain directly into the watershed (via impervious surfaces) and is instead directed onto pervious surfaces. The concept of EIA corrects for the second problem by excluding disconnected impervious surfaces from the determination of imperviousness. EIA is a subset of TIA, and lacks the incorrect assumption that all impervious surfaces contribute to runoff. However, as they point out, the direct measurement of EIA is complicated, even with sophisticated tools such as GIS, which is likely the reason this discussion is absent from much of the earlier research. Because of these inconsistencies Booth and Jackson (1997) argue that any conclusions drawn from the comparison of these studies, including the assertion of important watershed imperviousness thresholds, will have limited precision.

Additionally, more recent research and analyses do not clearly support earlier generalizations about watershed imperviousness thresholds. Instead, they provide evidence that declines in environmental indicators that accompany increases in imperviousness are more

complicated, but loosely follow a linear pattern. For instance, Karr and Chu (2000) demonstrate that the environmental health (as measured by an index of biological integrity) of a watershed is negatively correlated with increasing % TIA, and no clear thresholds are apparent. Instead they assert that while TIA is important in determining some of the impacts of urbanization on a watershed, it does not sufficiently capture all of the effects of urbanization. While highly impervious watersheds were uniformly poor, the variation in watershed health increased as imperviousness declined. They conclude that local conditions and variables (riparian cover, point source pollution, etc) are not entirely captured by TIA, and the assumption of a tight and simple relationship between TIA and environmental health indicators should be abandoned.

While much of the investigation of watershed imperviousness has focused on ecological indicators like species diversity and habitat quality, there have also been studies that focus specifically on the relationship between imperviousness and NPS pollution. Interestingly, while much of the more recent research makes some mention of watershed imperviousness thresholds, results supporting the hypothesis of imperviousness thresholds being an important driver of NPS pollution are largely absent. However, similar to research concerned with the increasing hydrological and ecological impacts caused by increasing imperviousness, many of the studies do support the hypothesis that there is a clear relationship between increasing imperviousness and increasing NPS pollution. Additionally, other variables associated with urban land use, such as household density, population density and access to and type of sewer and drainage infrastructure have also been correlated to storm water contamination and loading of surface waters (Carle et al, 2005; Frenzel and Couvillion, 2002; Mallin et al, 2001).

Although there is a growing consensus that urbanization and elevated levels of watershed surface imperviousness result in greater loading of NPS pollutants, the effect of urbanization on

temporal intra-storm loading patterns remains the focus of considerable research and debate. Understanding the distribution of NPS pollutant mass as it relates to stormwater volume is important because it can inform watershed management and the implementation of appropriate BMPs. Structural measures that are built to reduce the water quality impacts of NPS pollution, such as sedimentation basins are often designed to mitigate the “first flush” of stormwater runoff. The first flush hypothesis describes a situation where a disproportionately large fraction of total NPS pollutant load is delivered to receiving waters during the initial phase of stormwater runoff. The primary mechanism proposed for this phenomenon is that pollutants that have accumulated between storms, particularly those on impervious surfaces, are quickly washed off by the earliest stage of a rain event. Thus, the first flush hypothesis predicts that impervious surfaces not only increase total NPS pollutant load, but also affect the timing and distribution of loading that occurs in more heavily developed and urbanized watersheds.

Research testing the first flush hypothesis has produced a variety of often conflicting results. The earliest studies were generally hampered by vague and qualitative definitions of what constituted the phenomenon (Goonetilleke et al, 2005), making comparisons of results between different projects difficult, if not impossible (Dilectic, 1998). Furthermore, sampling designs often differed depending on the NPS pollutant in question and the scale of the study location. However, Bertrand-Krajewski et al (1998) proposed both a standard methodology and quantitative definition for the first flush phenomenon that has since been widely accepted by other researchers. They used a dimensionless mass vs. volume curve where cumulative pollutant mass is divided by the total pollutant mass and plotted in relation to the cumulative volume divided by the total volume. These M/V curves show the distribution of pollutant mass over the course of a storm, and correct for variable factors such as length of storm and total discharge, making possible comparisons between

different storm events and watersheds. Additionally, they defined the first flush phenomenon as occurring when 80% of total pollutant mass was delivered by the initial 30% of total flow.

Results meeting the 80%/30% rule have come almost exclusively from research examining NPS pollutants such as heavy metals, organic compounds and nutrients (Tiefenthaler et al, 2008; LI et al, 2007, Stein et al, 2007; Lee et al, 2004; Lee et al, 2002; Line et al, 1997). Although similar investigations of microbial NPS pollutant loading have been attempted (Stumpf et al, 2010; Krometis et al, 2007; Surbeck et al, 2006) there is little evidence to support for the first flush effect's occurrence with these contaminants. Instead these results indicate that loading of fecal indicator bacteria remains relatively constant over the course of storms, regardless of watershed surface imperviousness.

Studies have also identified potential links between storms and the outbreak of waterborne disease in human populations (Drayna et al, 2010, Craun et al, 2005; Curriero et al, 2001). More than 140 waterborne microorganisms have been identified as pathogens, including *Giardia*, *Pseudomonas*, *Listeria*, *Campylobacter*, *Shigella*, *Naegleria*, *Cryptosporidium* and *Escherichia coli* O157:H7 (Reynolds et al, 2008). While researchers have described 100s of waterborne disease outbreaks in the United States, existing surveillance is thought to grossly underestimate the actual public health impact of these diseases (Yoder et al, 2008; Reynolds 2008). A recent study estimated an incidence of 16.4 million cases of acute gastroenteritis per year attributable to drinking water sources in the United States (Messner et al, 2006). Understanding how watershed land use influences both dry-weather and storm event microbial NPS pollution will potentially aid regulators responsible for mitigating the public health risks of surface water sources of drinking water.

Study Area

Durham and Chapel Hill are located in the Piedmont region of Central North Carolina and together with the city of Raleigh, define the boundaries of The Research Triangle Area (Figure 1). The local geography is characterized by well formed low lying hills; with elevations ranging from 75 to 200 m above sea level. Soils are primarily low permeability clays, which contribute to runoff during storm events and low flow levels during periods of dry weather (NCDENR, 2005). Like many other urban areas in the United States of America, The Triangle is undergoing rapid growth that typically takes the form of low-density residential and commercial development that uses land at a rate greater than population growth. From 1950-2000, the Triangle's urban population increased 480% while the urban land area increased 1,670% (TJCOG 2008). This pattern of development is associated with relatively high levels of impervious cover, including roads, parking lots and roofs; impairment and degradation of nominally pervious surfaces and both centralized and distributed wastewater infrastructure; all of which contribute to increased NPS pollution to area surface waters.

While there is an increasing need to understand the magnitude, distribution and timing of microbial contamination of surface waters, especially those used as municipal sources (NRC 2008a, 2008b; NSTC-SWAQ 2007); these parameters have yet to be fully characterized. This is particularly true of inland surface waters. Much of the research linking urban development and nonpoint source contamination has been limited to coastal areas (Stumpf et al, 2010; DiDanato, 2009; Coulliette et al, 2009; Mallin et al, 2001). While there have been a handful of studies that have focused on the inland surface waters of urbanized watersheds, most examine nutrient contamination exclusively (Shields et al 2008; Groffman et al 2004; Hatt et al, 2004; Band et al 2001) or were conducted in areas that make comparisons to the Southeastern United States difficult (Sinclair et al, 2009, Frenzel and Couvillion, 2002; Kistemann et al, 2002).

Objectives

The primary objectives of this study are (1) to analyze the magnitude, timing and intra-storm loading distribution of microbial contaminants at sites upstream of Jordan Lake, a drinking water source and (2) to relate loading and sample concentration of microbial contaminants to specific land use and impervious surfaces. A better understanding of the influence of urban development on microbial contamination of North Carolina inland surface waters will contribute to the knowledge needed to bring these waters into compliance with state standards. Furthermore, these methods will be applicable to inland watersheds nationwide.

Materials and Methods

Site Selection

This study examined 15 sites on Morgan Creek, New Hope Creek and North East (NE) Creek tributaries (Table 1). All of these stream reaches are within the B. Everett Jordan Lake catchment. Jordan Lake is the largest reservoir within the Cape Fear River Basin, covering approximately 13,940 acres. The reservoir was formed by damming the Haw River, Morgan Creek, New Hope Creek and NE Creek in 1981 and is operated by the U.S. Army Corps of Engineers for flood control, water quality (downstream low flow augmentation), fish and wildlife conservation, recreation, and water supply.

To the extent possible we located our sampling locations at preexisting monitoring sites (Chapel Hill, Durham, NCCOOS, USGS, EPA/NCDNR). Of these, 8 of the 15 sites were placed at or near gages that measure streamflow. Additionally, we made an effort to select sites with watersheds that account for variation in land use, impervious surface cover and watershed area (Figure 1).

Impervious Surfaces and Land Use

We utilized the ArcGIS software package and the Arc Hydro Toolbox to delineate watershed boundaries above the selected sites and determine land cover and watershed area. We based land cover characteristics on the 2006 Multi-Resolution Land Characterization Consortium's National Land Cover Data (Homer et al, 2004; Homer et al, 2007). This land cover data set is the most recent available that covers the full extent of the study area. The NLCD impervious surface data divides land surface into a grid with a resolution of 30 m. These 30 x 30 m 'pixels' are classified with one of 101 possible values (0% - 100%), representing the percent impervious surface coverage. Pixels were tabulated for each of the impervious surface values and summed to get the total number of pixels in the watersheds. For each of the 15 upstream watersheds, total surface imperviousness percentage was calculated by summing impervious surface pixel values and dividing by total number of pixels counted in the watershed. Upstream watershed percent development, forest and agriculture cover were calculated by tabulating and grouping assigned values and dividing by total watershed area.

Sites were divided into three levels of development intensity, as measured by % IS in the watershed upstream of each sampling point. The five sites with the lowest % IS were assigned to the 'Low intensity' development class (0.5 to 4.0%), the five sites with intermediate % IS were assigned to the 'Intermediate intensity' class (4.1 to 14 %) and the five sites with the largest % IS were assigned to the 'High intensity' class (15 to 34%).

Watershed Area

Sites were divided into three categories of watershed size as measured by area in hectares (ha). The five sites with the smallest area were assigned to the 'Small' watershed size category (142 to 1,224 ha), the five sites with intermediate areas were assigned to the 'Medium' category (1,384

to 5,463 ha) and the five sites with the largest areas were assigned to the 'Large' category (5,847 to 19,734 ha).

Precipitation and Stream Flow

We retrieved hourly precipitation data from the National Oceanic and Atmospheric Administration's U.S. Climate Reference Network (USCRN, 2011) Durham station. We also made an attempt to use precipitation data collected by the NC COOS gauges at two of the sample sites, but evaluation revealed that these data were inconsistent and inaccurate due to continued insect infestation of tip buckets. Antecedent precipitation was calculated for each sample time by independently summing the preceding 2, 24, 48 and 168 hourly observations.

Six of the sites were located at USGS gages that collect stream flow rate data four times an hour. Stream flow rate was determined by matching sample collection time with the most proximate USGS gage observation time. An additional two sample sites were located at NC COOS gages that collect stream flow rate data four times an hour. However, the gage at Crow Branch Creek was prone to malfunction, and these stream flow data were not included in our analysis. Stream flow rates at the remaining NC COOS site were determined in the same manner as at the USGS sites.

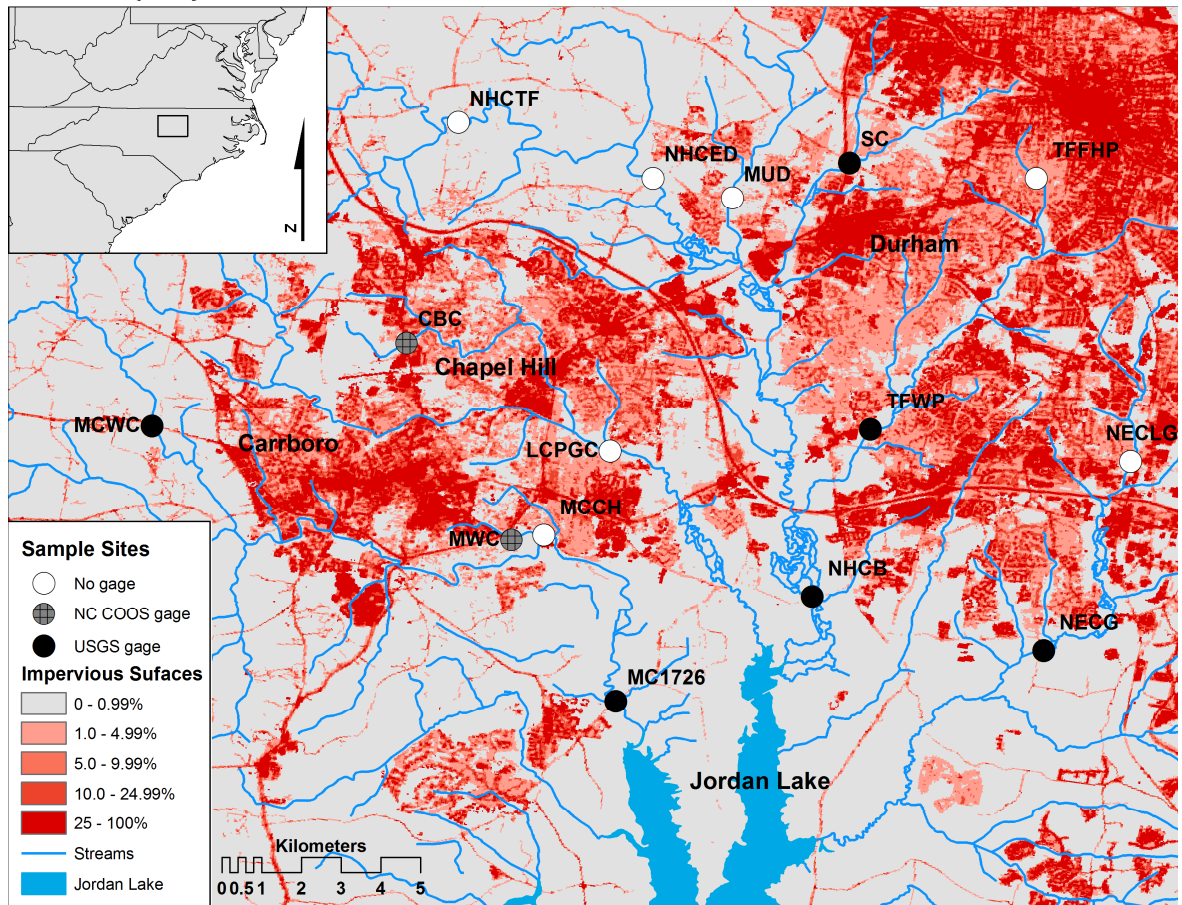
Table 1: Study sites

Site Name	Abbr.	^a Trib.	Gage	Watershed Area (ha)	Developed (%)	Agricultural (%)	Forested (%)	^b IS (%)	^c DI
Morgan Creek at NC-54 West (White Cross)	MCWC	MC	USGS	2,198	5.3	23	72	0.5	L
Meeting of the Waters Creek	MWC	MC	NCCOOS	231	86	0	14	34	H
Morgan Creek near Chapel Hill	MCCH	MC	USGS	10,420	18	15	66	4.0	L
Little Creek at Pinehurst Golf Course	LCPGC	NHC	No	4,930	55	4.6	39	10	I
Morgan Creek at NC-1726	MC1726	MC	No	12,009	19	14	64	4.1	I
New Hope Creek at NC-1107 (Blands)	NHCB	NHC	USGS	19,734	40	8.3	46	8.8	I
Northeast Creek at SR1100 (Genlee)	NECG	NEC	USGS	5,463	57	4.7	34	14	I
Northeast Creek at SR1182 (Lowes Grove)	NECLG	NEC	No	779	67	2.3	30	15	H
Third Fork NHC at Woodcroft Parkway	TFWP	NHC	USGS	3,840	85	0.8	9.8	18	H
Third Fork Creek NHC at Forest Hills Park	TFFHP	NHC	No	151	99	0	0.7	17	H
Sandy Creek at Cornwallis Rd	SC	NHC	USGS	1,224	79	0.9	20	22	H
Mud Creek at NC 751	MUD	NHC	No	1,384	35	11	52	5.0	I
New Hope Creek at Erwin Road	NHCE	NHC	No	8,166	7.8	15	76	1.1	L
New Hope Creek at Turkey Farm Road	NHCTF	NHC	No	5,847	8.3	17	73	1.3	L
Crow Branch Creek at MLK	CBC	NHC	NCCOOS	142	12	10	77	3.6	L

^aMC - Morgan Creek, NHC – New Hope Creek, NEC – North East Creek ^bIS – Impervious surface coverage.

^cDI- Development Intensity: L - Low intensity (0.5 to 4.0% IS), I - Intermediate intensity (4.1 to 14% IS), H - High intensity (15 to 34% IS).

Figure 1: Study area showing sampling points and the New Hope Creek branch of Jordan Lake, N.C. (USA).



Sample sites are labeled as follows: MCWC - Morgan Creek at NC-54 West (White Cross); MWC - Meeting of the Waters Creek at Laurel Hill Rd.; MCCH - Morgan Creek near Chapel Hill; LCPGC - Little Creek at Pinehurst Golf Course; MC1726 - Morgan Creek at NC-1726; NHCB - New Hope Creek at NC-1107 (Blands); NECG - Northeast Creek at SR1100 (Genlee); NECLG - Northeast Creek at SR1182 (Lowes Grove); TFWP - Third Fork NHC at Woodcroft Parkway; TFFHP - Third Fork Creek NHC at Forest Hills Park; SC - Sandy Creek At Cornwallis Rd; MUD- Mud Creek at NC 751; NHCE- New Hope Creek at Erwin Road; NHCTF -New Hope Creek at Turkey Farm Road; CBC - Crow Branch Creek at MLK.

Sampling Design

Dry-weather Sampling

Background dry-weather (DW) samples were collected bimonthly between April, 2010 and March, 2011. A total of 301 samples were collected on 22 days. The total included 45 samples after

a statistical test showed FIB concentrations did not differ significantly from the regularly collected samples. These pre-storm samples took the place of dry-weather samples that would have been collected the same week had there been no storm. Crow Branch Creek, Third Fork Creek at Forest Hills Park and New Hope Creek at Turkey Farm Road ran dry at times over the sampling period. Samples were not collected if water was not running in the creek bed. Also, 9 dry-weather samples were not collected because the streams at the sample points were frozen. Sampling was delayed if precipitation in excess of 2.5 cm had occurred in the 72 hr period preceding planned collection. Grab samples for microbial assays were collected in autoclaved 1 L polypropylene bottles from each of the sites. Most samples were collected by lowering empty sample bottles in a secure cage from an over passing bridge or causeway (Figures 27 and 28). However, in the event of hazardous traffic conditions, samples were collected by wading out to midstream. In both cases, efforts were made to sample in an upstream fashion to minimize the collection of disturbed sediments. Once water samples had been collected, a YSI Professional Pro was used to record water temperature, dissolved oxygen, conductivity, total dissolved solids and pH. Microbial samples were immediately placed on ice until processing, which always occurred within 6 hrs of collection. A bench-top Hach 2100N nephelometer was used to determine turbidity once the samples had been returned to the lab.

Storm Event Sampling

We defined storm sampling events as at least three days without appreciable rainfall followed by a rainfall event that was anticipated to increase stream flow at least four times (4 X) over pre-storm rates. Over the course of each storm, 4 grab samples were collected from each of the 15 sites. The first sample was collected just prior to initial precipitation. The second sample was collected between 2-4 hours after the onset of precipitation. The third sample was collected between 5-12 hrs after initial precipitation, or as close to peak stream flows as possible. The fourth sample was collected between 12-36 hrs after initial precipitation.

Samples were collected in the same manner as during the dry-weather events, with two notable exceptions. The first was that all samples were collected by lowering empty bottles from bridges or causeways. The second was the inclusion of an additional 500 ml polypropylene bottle. Before being sealed and placed on ice, field technicians used a digital thermometer to record the temperature of the water sample held in the 500 ml bottle. Once the samples had been returned to the lab, the contents of the 500 ml bottle were tested with a YSI Professional Plus to determine other physical parameters. Sample processing occurred within 6 hrs of collection for all samples, except during the second storm, where logistical problems delayed the FC assays 12-36 hours. During this time samples were kept sealed in the dark and on ice.

Detection of Indicator Species

Both FC and EC concentrations were determined following the standard membrane filter methodology (APHA, 1998). Briefly, samples were filtered through membranes, placed onto selective media (mFC and M-TEC) and allowed to incubate for 18-24hrs before enumeration. Sample volumes varied from 0.5-100 ml and three different volumes of each sample, based on anticipated FIB concentrations, were filtered for both FC and EC assays. Plates were enumerated visually and counts greater than 350 colonies were excluded as too numerous to count. FIB concentrations (colony forming units (CFU)/100 ml) were determined by taking a weighted average of plate counts for each sample.

Statistical Methods

All statistical analyses were performed using Microsoft Excel or the R statistical computing language (R Development Core Team, 2010). FC and EC indicator concentrations were analyzed independently. All FIB concentration data were $\log_{10}(x + 1)$ transformed before analysis to meet statistical criteria for normality and homoscedasticity.

An Excel linear interpolation function was used to estimate FIB concentrations between samples (adapted from Stumpf et al, 2010). Total storm event loading was calculated by multiplying streamflow volume per 15 minute period by measured or interpolated FIB concentration (CFU/100 ml) and summing over the extent of the storm. The start of storm events was considered to be the time at which precipitation began. The end of storm events was determined by visually inspecting individual stream hydrographs and identifying the time at which streamflow stabilized into new baseflow equilibrium. Dry-weather loading periods were defined as the 24 hrs following sample collection, except for the final sample where the 24 hrs directly preceding sampling served as the basis for the calculation. Dry-weather loading was calculated by multiplying streamflow volume per 15 minute period by measured or interpolated FIB concentration (CFU/100 ml) and summing over the 24 hr period.

The effects of sample type, watershed imperviousness and watershed area on FIB concentrations were evaluated using a 3-factor analysis of variance, with sample type, watershed imperviousness and watershed area as fixed factors. First order interaction terms were excluded from the final model if non-significant. Post hoc Tukey pair wise comparisons were used on significant factors to determine factor level differences.

Results and Discussion

Physical and Chemical Parameters

Creek water temperature ranged from 0.7 to 26.6 °C during the study period. Dissolved oxygen was lower during dry-weather (6.3 ± 2.8 ppm) than during storm events (8.1 ± 1.7 ppm). Other measured parameters were also greater during storm events than during dry-weather,

including turbidity, TDS and streamflow (Table 24). Measures of pH, conductivity and water temperature were all lower during storm events than during dry-weather.

Loading Analysis and Characterization

Precipitation duration, cumulative precipitation and FIB loading demonstrated considerable inter-storm variation (Table 2). The first storm, the remnant of tropical depression Nicole, was the longest in duration and produced the greatest amount of precipitation. Measures of total loading as the result of the first storm were several orders of magnitude greater than either of the other storms and both FC and EC EMCs were correspondingly higher.

Individual creek hydrographs showed the clearest reaction to the first storm (Figure 8). During the first storm, all gauged creeks responded with greater than 4-fold increases in stream flow volume.

Table 2: Storm event precipitation statistics and storm event FIB loading, all creeks combined

Event	Date	Precipitation duration (hrs)	Cumulative precipitation (cm)	Total Loading (CFU/storm)		EMC (CFU/100 ml)	
				FC	EC	FC	EC
Storm 1	9/29/2010	32	9.84	1.10×10^{14}	1.33×10^{13}	8,517	1,886
Storm 2	11/16/2010	15	0.76	3.61×10^{11}	1.08×10^{11}	1,181	320
Storm 3	01/17/2011	7	0.28	5.26×10^{10}	5.09×10^{10}	143	138
Storm Average	-	18	3.63	3.69×10^{13}	4.50×10^{12}	3,280	781

While both the second and third storms were forecast to deliver greater than 1.0 cm of precipitation, both fell short of these levels and in turn, only some creeks reached the anticipated 4-fold increase in stream flow volume (Figures 9-10). Although the second and third storms were smaller in magnitude than expected, the frequency of these smaller storms in central North Carolina is much greater than precipitation events comparable to the first storm. Despite much lower

measures of precipitation and duration, these smaller storms were still capable of delivering FIB loads equivalent to days or weeks of average dry-weather loading (Tables 15-21).

Dry-weather FIB loads demonstrated considerable seasonal variation. Both FC and EC dry-weather loading per 24 hour period (day) was an order of magnitude greater during spring months in comparison to all other seasons (Figure 11). Average daily spring FC loads were equivalent to loading occurring over 4.3 average summer days, 7.7 autumn days and 4.2 winter days. Average daily spring EC loads were equivalent to loading occurring over 3.8 average summer days, 7.6 autumn days and 1.4 winter days. EC loads were less than FC loads in all season, except winter, when they were slightly higher (Table 3).

Table 3: Seasonal dry-weather FIB loading, all creeks combined

Season	Total Loading (FC CFU/24 hrs)	Total Loading (EC CFU/24 hrs)	EMC (FC CFU/100 ml)	EMC (EC CFU/100 ml)
Spring (n = 33)	3.79×10^{11}	2.10×10^{11}	920	541
Summer (n = 36)	8.84×10^{10}	5.51×10^{10}	547	284
Autumn (n = 24)	4.95×10^{10}	2.77×10^{10}	160	98
Winter (n = 37)	9.05×10^{10}	1.49×10^{11}	184	161
Average	1.55×10^{11}	1.16×10^{11}	467	280

Average storm event loading of both FC and EC greatly surpassed average 24 hour dry-weather loading at all creek sites (Table 4). FC event loading was consistently greater than EC event loading. The average storm event FC load was equivalent to 237 days of dry-weather loading. The average storm event EC load would require 39 days of dry-weather loading (Figure 12). The greatest differences between storm event and dry-weather loading of FC were at NHCB and TFWB, respectively. TFWB and SC had much higher dry-weather to storm EC loading ratios than the remaining sites. The smallest difference between storm event and dry-weather loading of FC and EC was at MC1726.

Table 4: Average dry-weather (DW) and average storm event FIB loads for all creeks and equivalent days of dry-weather necessary to equal event loading of both FC and EC.

Creek	FC Loading			EC Loading		
	DW (CFU/24 hrs)	Storm (CFU/Storm)	DW days	DW (CFU/24hrs)	Storm (CFU/Storm)	DW days
MCWC	9.25×10^9	1.43×10^{12}	154.3	5.58×10^9	5.78×10^{11}	103.7
MWC	1.51×10^{11}	2.45×10^{13}	162.3	9.82×10^{10}	3.05×10^{12}	31.0
MC1726	2.02×10^{11}	1.30×10^{13}	64.7	1.79×10^{11}	3.81×10^{12}	21.3
NHCB	4.50×10^{11}	1.72×10^{14}	382.2	3.81×10^{11}	8.90×10^{12}	23.3
NECG	1.29×10^{11}	2.05×10^{13}	158.5	5.46×10^{10}	4.79×10^{12}	87.7
TFWB	5.91×10^{10}	1.92×10^{13}	316.7	3.78×10^{10}	7.73×10^{12}	188.5
SC	3.45×10^{10}	7.61×10^{12}	220.5	1.23×10^{10}	2.62×10^{12}	213.5
All creeks combined	1.55×10^{11}	3.69×10^{13}	237.3	1.16×10^{11}	4.50×10^{12}	38.8

Event Mean Concentration (EMC) is defined as total pollutant mass (M) divided by total stream flow volume (V) and eases comparisons between different creeks and storms by correcting for variable stream flow and storm duration (Bertrand-Krajewski et al, 1998). Storm FC EMCs were as much as 20.6 times greater than during dry-weather, while storm EC EMCs were as much as 10.4 times greater than dry-weather EMCs (Table 5). The average combined storm event FC EMC was 7.0 times greater than the corresponding average dry-weather FC EMC.

Table 5: Dry-Weather (DW) and storm event mean concentrations (EMC) for all creeks and one way ANOVA test results.

Creek	EMC (FC CFU/100 ml)			EMC (EC CFU/100 ml)		
	DW	Storm	Storm/DW	DW	Storm	Storm/DW
MCWC	256	3,646	14.2	143	1,494	10.4
MWC	386**	4,389**	11.4	237	537	2.3
MC1726	581	1,685	2.9	528	517	1.0
NHCB	294	6,052	20.6	208	322	1.5
NECG	270	1,525	5.6	127	404	3.2
TFWB	525	2,439	4.6	376	1,087	2.9
SC	956*	3,224*	3.4	350	1,109	3.2
All creeks combined	467*	3,280*	7.0	289**	781**	2.7

*Significant at $p < 0.05$, **Significant at $p < 0.01$.

The average combined storm event EC EMC was 2.7 times greater than the average dry-weather EC EMC. All storm event EMCs were greater than dry-weather EMCs, except at MC1726, which had a slightly higher EC EMC during dry-weather than during storms. Log-transformed dry-weather and storm FC EMCs differed significantly at MWC ($p < 0.01$), SC ($p < 0.05$) and when all creeks were combined ($p < 0.05$). EC EMCs did not differ at the level of individual creeks, although differences between storm and dry-weather EMCs were significant ($p < 0.01$) when all creeks were combined.

Pollutant Mass to Volume Curves

Individual creek mass to volume (M/V) curves were calculated to determine the pattern and distribution of both EC and FC loading per volume of streamflow during each of the three sampled storms (Figures 13-26). Of 42 FIB M/V curves only one reached the 80%/30% mass: volume first flush threshold. The FC M/V curve at MCWC during the second storm demonstrated a strong first flush loading pattern (Figure 13) and delivered 81.4% mass FC during the initial 30% storm runoff volume. The EC M/V curve at MCWC during the second storm weakly followed this loading pattern, but did not meet the 80%/30% threshold; delivering 80% mass EC after the initial 58.2% volume (Figure 14).

Average M/V curves for each creek indicate that loading of both FC and EC remains relatively constant over the course of storms (Figure 2). Averaged individual creek FC and EC loading after the initial 30% runoff volume for all storms was 27.3% and 27.4% of total mass, respectively (Table 6). The average creek data do not provide evidence to support first flush loading of either FC or EC pollutants in the sampled watersheds. Interestingly, the two creeks with the greatest initial average FC and EC loading, MCWC and MWC, differ considerably in watershed land use and impervious surface coverage (Table 1).

Figure 2: Average mass to volume (M/V) curves for (A) FC and (B) EC at each gauged creek site.

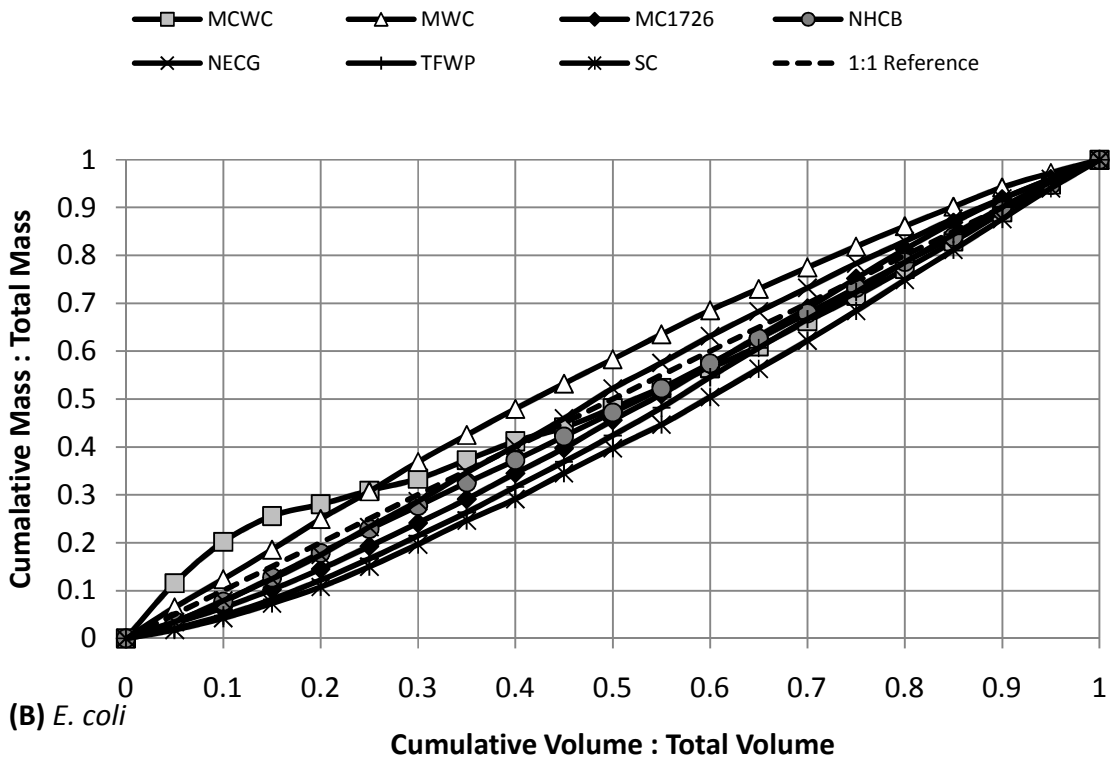
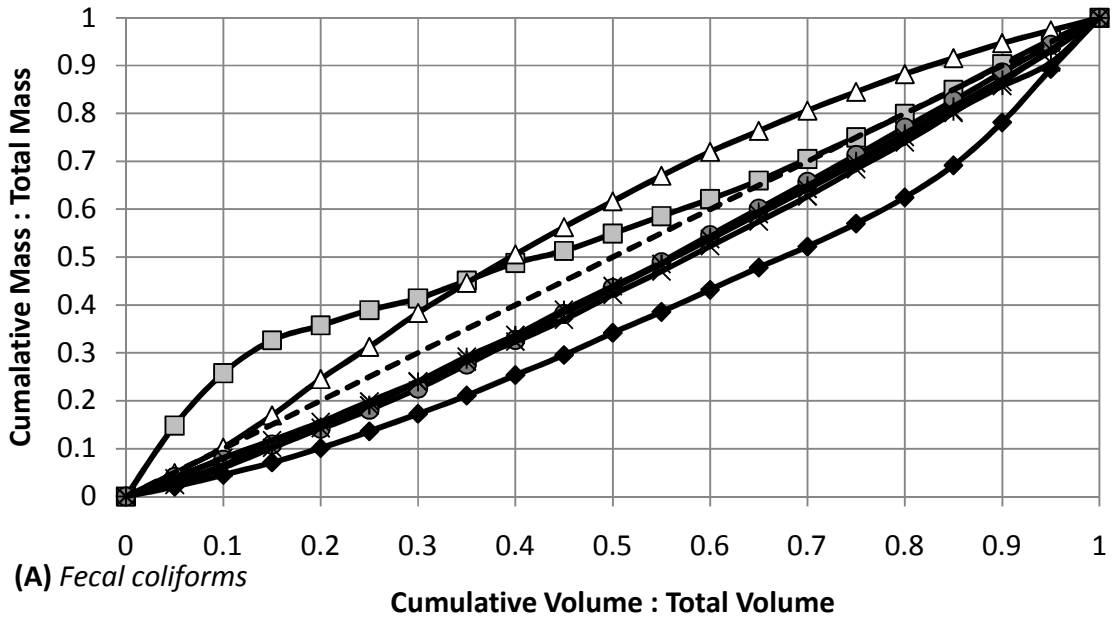


Table 6: Range and average of FC and EC mass loading after initial 30% volume storm runoff for individual creeks and all creeks combined.

Creek	FC		EC	
	Range	Average	Range	Average
MCWC	10.8 - 81.4%	41.4%	8.1 - 66.6%	33.4%
MWC	30.1 - 43.2%	38.3%	31.5 - 44.8%	36.9%
MC1726	13.4 - 21.7%	17.3%	20.7 - 29.6%	24.1%
NHCB	12.4 - 29.2%	22.5%	22.9 - 32.2%	27.7%
NECG	14.6 - 32.5%	23.9%	24.0 - 31.3%	28.6%
TFWP	14.9 - 33.2%	23.9%	16.6 - 24.4%	21.4%
SC	18.0 - 31.8%	24.0%	15.7 - 22.9%	19.6%
All creeks combined	10.8 - 81.4%	27.3%	8.1 - 66.6%	27.4%

The watershed upstream of MCWC is predominantly forested (71.5%) and has the least impervious surface coverage (0.5%) of all sampled watersheds. In contrast, the MWC watershed contains the main campus of the University of North Carolina at Chapel Hill and is highly developed (85.7%). Additionally the MWC watershed has the greatest impervious surface coverage (34.0%) of all sampled watersheds.

These results are largely consistent with other studies that have found no strong pattern of first flush loading of microbial contaminants (Stumpf et al, 2010; Krometis et al, 2007; Surbeck et al, 2006). Krometis et al (2007) sampled two creeks in central North Carolina (including MWC), and although they reported that neither FC or EC loading fulfilled the 80%/30% rule, they did note that the largest proportion of settleable, particle-associated FIB were contained in the first 50% of runoff volume. However, other comparisons between our results and the loading patterns observed by Krometis et al (2007) are difficult to make because they did not report combined settleable and suspended FIB M/V curves and we did not distinguish FIB based on particle association.

The Stumpf et al (2010) study of North Carolina headwater tidal creeks provides another example of FIB loading patterns that do not meet the criteria for the first flush effect. However, they conclude that this is likely the result of light development and low levels of impervious surface

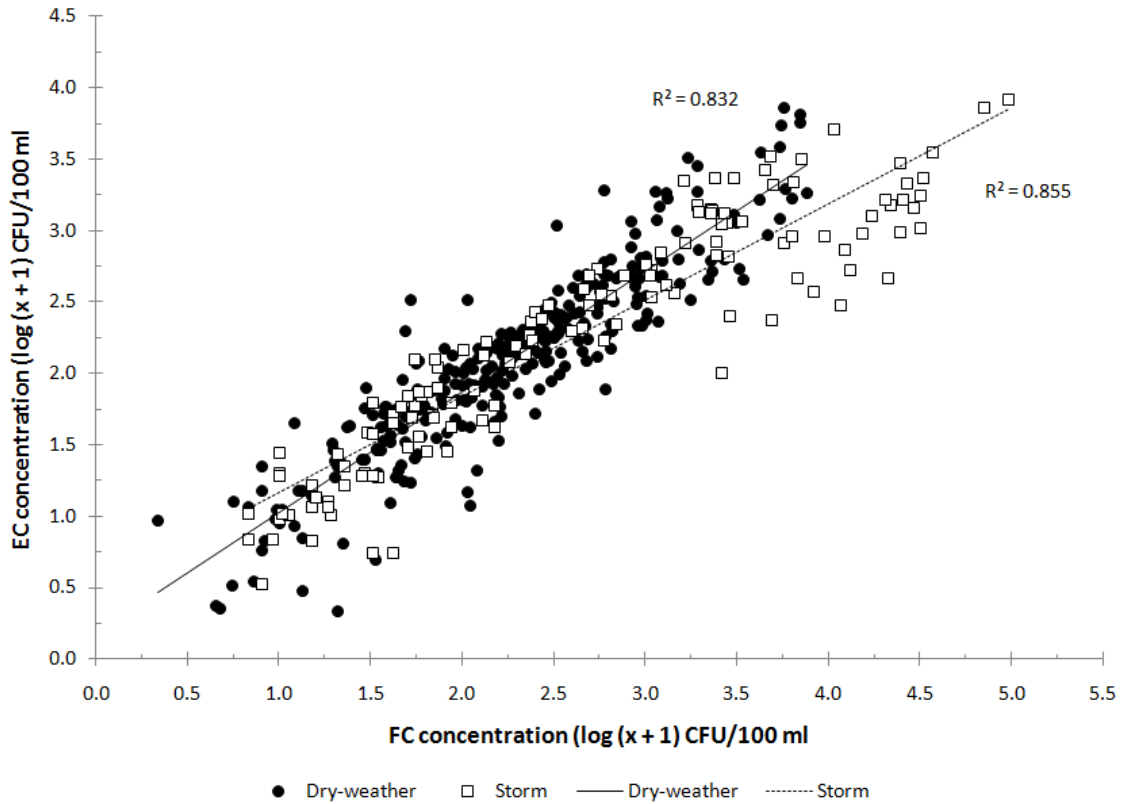
coverage in the watersheds they examined. While we also failed to observe the first flush effect, we cannot provide the same caveats as we sampled watersheds that had a wide variety of land use characteristics and impervious surface coverage.

Likewise, the Surbeck et al (2006) study of creeks in southern California did not produce results that support the first flush loading effect. Interestingly, they suggest that the “buildup/wash off” paradigm on which the first flush hypothesis is based may be inadequate to describe loading patterns of microbial NPS pollutants. While it may be a satisfactory model for pollutants such as nutrients, organic compounds and heavy metals, they point to several studies that indicate that environmental reservoirs of bacteria may contribute to concentrations of FIB in surface water (Byappanahalli et al, 2003, Solo-Gabriele et al, 2000; Fujioka et al, 1999). Under the “mud puddle” hypothesis they propose, FIB concentrations are more or less constant everywhere in the environment and uniformly partition into runoff over the course of storm events. Surface imperviousness may affect hydrology and runoff patterns, but if FIB concentrations are constant, no first flush effect will be observed. Instead, FIB mass loads will simply mirror stream flow discharge and M/V curves will remain relatively flat. While our loading results are consistent with the mud puddle hypothesis, additional research on the persistence and potential replication of FIB in North Carolina surface waters should help to clarify the causes of these loading patterns.

FIB Concentration Patterns

Fecal indicator bacteria concentrations of FC and EC were highly correlated for any given sample (Figure 3).

Figure 3: Correlation between log-transformed FC and EC concentrations during both dry-weather and storm events. *Pearson's correlations significant at $p < 0.001$.



Pearson's correlations were used to determine that the relationship between log-transformed FC and EC concentrations during both dry-weather and storm events. Correlations for both dry-weather and storm samples were positive, linear and statistically significant.

Dry-Weather and Storm Event FIB Concentrations

Overall FC concentrations ranged from 1.2×10^0 to 9.72×10^4 colony forming units (CFU)/100 ml while measures of EC tended to be lower, ranging from 1.2×10^0 to 8.28×10^3 CFU/100 ml (Table 7). Measurements of FIB followed a pattern of increasing concentrations over the course of storms.

Table 7: Summary statistics of FIB concentrations during dry-weather and storm events, all creeks combined.

	Range	Median	Mean	Std dev
FC dry - weather (n = 301)	$1.2 \times 10^0 - 7.65 \times 10^3$	173.8	600.5	1212.3
FC storm event (n = 135)	$5.88 \times 10^0 - 9.72 \times 10^4$	294.1	5267.8	12761.1
EC dry - weather (n = 301)	$1.2 \times 10^0 - 7.24 \times 10^3$	128.8	370.2	853.3
EC storm event (n = 135)	$2.35 \times 10^0 - 8.28 \times 10^3$	205.9	711.7	1237.7

Both FC and EC concentrations were greatest during the peak and falling stages of the storms (Figure 4, Table 8). A one-way ANOVA pair wise comparison of means was used to test for differences in FIB concentrations across all storms at all creeks for samples captured during each of the four stages of the hydrograph (pre-storm, rising limb, peak and falling limb) and during dry weather base flow. FC concentrations differed significantly by sample type, $F(4, 431) = 6.50$, $p = 4.34 \times 10^{-5}$.

Figure 4: Summary box plots of log-transformed FC (left) and EC (right) concentrations across all creeks and all storms.

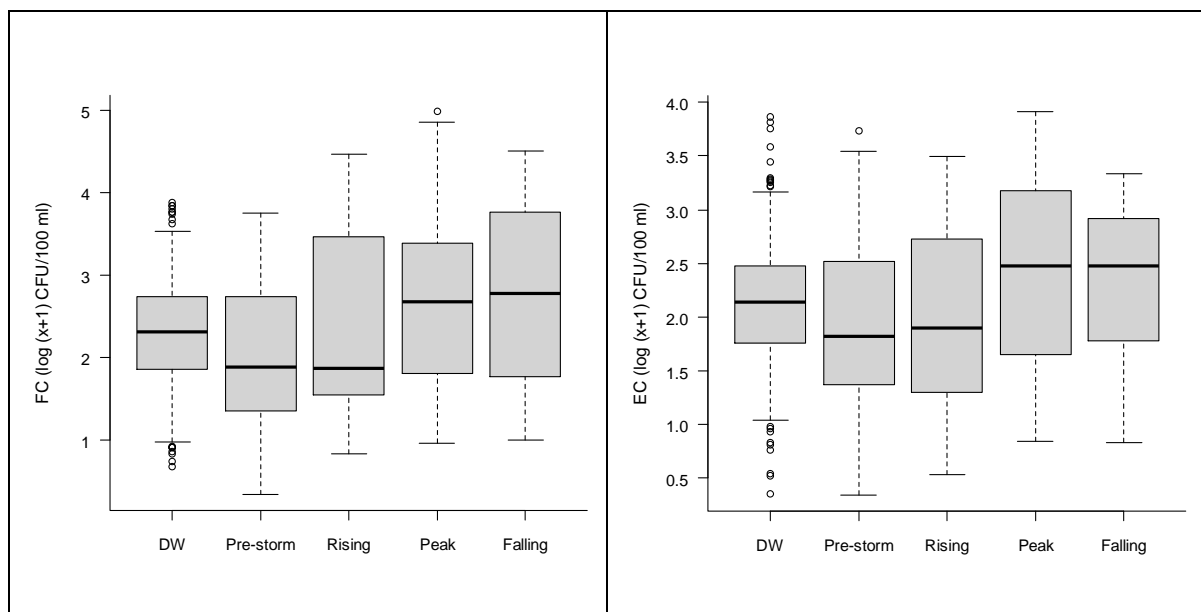


Table 8: Summary statistics of dry-weather and storm event FIB concentrations (CFU/100 ml), all creeks and all storms combined.

		Sample Type					
		Dry-weather n = 256	Pre-storm n = 45	Rising n = 45	Peak n = 45	Falling n = 45	
FIB	FC	Mean	590.8	655.8	3,801.5	6496.3	5,505.8*
		Std dev	1,191.7	1,336.4	7,389.6	18,690.5	9,391.5
	EC	Mean	344.2	518.1	434.8	1,172.0*	528.2
		Std dev	846.4	1,080.2	720.6	1857.3	606.0

*Log-transformed concentrations were significantly greater than dry-weather at $p < 0.05$.

Tukey post-hoc pair wise comparisons indicate that the pre-storm sample, rising limb and peak did not differ significantly from dry-weather FC concentrations ($p = 0.26$, $p = 0.91$ and $p = 0.06$, respectively). However, the falling limb concentrations were significantly greater than dry-weather FC concentrations ($p = 0.003$). No pair wise comparisons of rising, peak and falling stages were significant at $p < 0.05$, but both peak and falling stage FC concentrations were significantly greater than pre-storm concentrations ($p = 0.003$ and $p = 0.0002$, respectively)

EC concentrations also differed significantly by sample type, $F(4, 431) = 7.01$, $p = 1.80 \times 10^{-4}$.

Like FC concentrations, Tukey HSD post-hoc pair-wise comparisons indicate that the pre-storm sample did not differ significantly from dry-weather ($p = 0.61$). However, unlike FC only the peak stage samples were significantly greater than dry-weather samples ($p = 0.04$). All other EC pair-wise comparisons had $p > 0.05$. For all additional analyses, pre-storm samples were treated as part of the dry-weather sample population.

Precipitation, Streamflow and Water Temperature

Measures of total precipitation, storm event duration, 2-hour, 24-hour, 48-hour and 7 day antecedent precipitation (AP) were highly variable between storms. Total precipitation ranged from 0.28 to 9.84 cm. Storm event duration ranged from 7 to 32 hours. Longer duration measures of AP

were moderately and positively correlated with both EC and FC concentrations (Tables 9 and 10). When all creeks were combined, there were significant correlations between both EC and FC concentrations and all measures of AP except for the 2-hr metric. At individual creeks no correlations between 2-hr AP and FC or EC were statistically significant. Longer duration measurements of AP were more strongly correlated with FIB concentrations. Across all watersheds, the strongest correlation was between 48 –hr AP and FIB concentrations, followed by 7 – day AP and then 24 – hour AP. All individual creek site correlations were positive, except for three exceptions, but none of these were significant at $p < 0.05$. At gauged creeks, correlations between streamflow (m^3/sec) and FIB concentrations were inconsistent. Three of seven creeks (NECG, TFWP and SC) demonstrated moderate correlations between FIB concentrations and streamflow, but the remaining four had flat responses. Interestingly, the three creek sites where these relationships were significant had higher measures of upstream surface imperviousness than the creeks where

Table 9: Spearman's rank correlations (R^2) of all creeks combined and individual creek sites for measures of streamflow (m^3/sec) and antecedent precipitation (mm) vs. EC concentrations ($\log_{10}(x + 1)$ CFU/100 ml)

Creeks	Streamflow	Antecedent precipitation			
		2 hr	24 hr	48 hr	7 day
All creeks combined	0.007	0.008	0.188**	0.376**	0.246**
MCWC	0.000	0.106	0.237**	0.359**	0.236**
MWC	0.003	0.009	0.248**	0.325**	0.088
MCCH	-	0.002	0.385**	0.314**	0.073
LCPGC	-	0.001	0.381**	0.570**	0.375**
MC1726	0.000	0.001	0.096	0.230**	0.091
NHCB	0.094	0.001	0.046	0.322**	0.195*
NECG	0.382**	0.029†	0.276**	0.427**	0.156*
NECLG	-	0.001	0.129	0.432**	0.364**
TFWP	0.416**	0.010	0.164*	0.450**	0.425**
TFFHP	-	0.019	0.436**	0.593**	0.365**
SC	0.406**	0.002	0.431**	0.717**	0.330**
MUD	-	0.003	0.192*	0.568**	0.344**
NHCE	-	0.002	0.140*	0.427**	0.290**
NHCTF	-	0.020	0.280**	0.489**	0.522**
CBC	-	0.008	0.212*	0.213*	0.276*

*Significant at $p < 0.05$; ** Significant at $p < 0.01$; †Negative coefficient of correlation

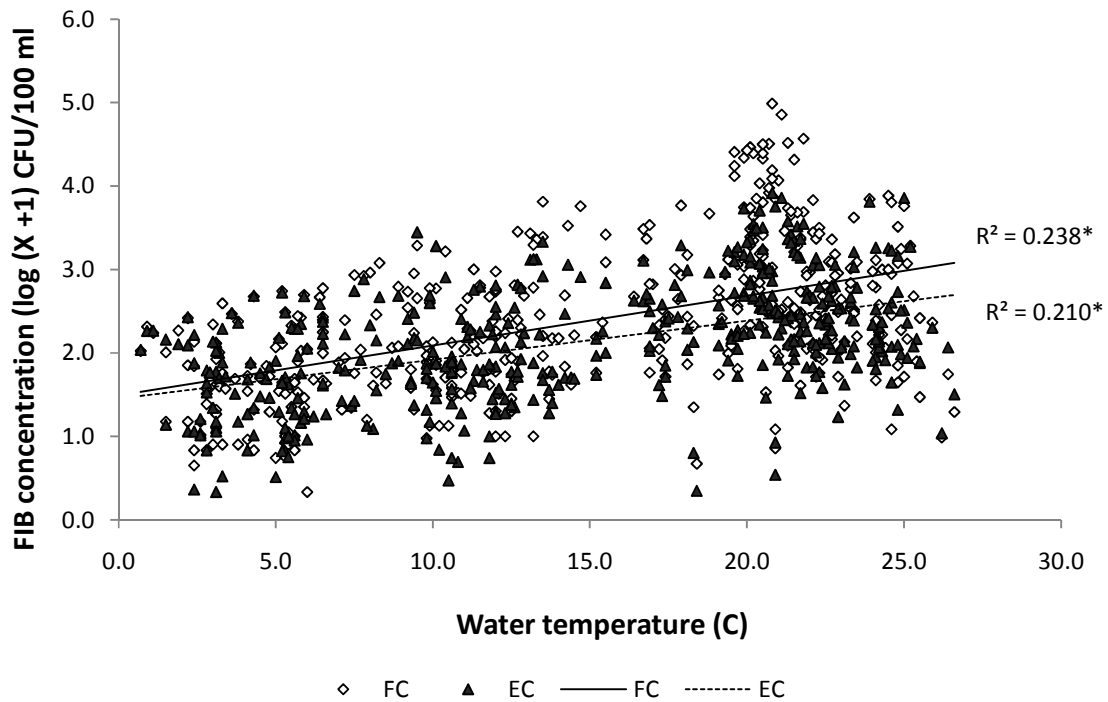
Table 10: Spearman's rank correlations (R^2) of all creeks combined and individual creek sites for measures of streamflow (m^3/sec) and antecedent precipitation vs. FC concentrations ($\log_{10}(x + 1)$ CFU/100 ml)

Creeks	Streamflow	Antecedent precipitation			
		2 hr	24 hr	48 hr	7 day
All creeks combined	0.020*	0.008	0.212**	0.419**	0.292**
MCWC	0.000	0.105	0.266**	0.339**	0.266**
MWC	0.004	0.004	0.392**	0.442**	0.196*
MCCH	-	0.008	0.417**	0.457**	0.196*
LCPGC	-	0.000	0.407**	0.633**	0.352**
MC1726	0.026	0.001†	0.109	0.334**	0.201*
NHCB	0.112	0.003	0.079	0.380**	0.208**
NECG	0.251**	0.013	0.168*	0.398**	0.245**
NECLG	-	0.001	0.205*	0.477**	0.396**
TFWP	0.390**	0.002	0.166*	0.459**	0.410**
TFFHP	-	0.014	0.391**	0.548**	0.343**
SC	0.328**	0.007	0.370**	0.589**	0.226**
MUD	-	0.000†	0.192*	0.615**	0.389**
NHCE	-	0.016	0.135*	0.390**	0.234**
NHCTF	-	0.028	0.201*	0.476**	0.530**
CBC	-	0.000	0.275*	0.339**	0.376**

*Significant at $p < 0.05$; ** Significant at $p < 0.01$; †Negative coefficient of correlation
streamflow correlations were not significant, although the creek with the highest measure of upstream impervious surfaces (MWC) did not follow this pattern.

The correlation results are consistent with observed intra-storm microbial loading patterns. Longer duration measures of AP correlate more strongly and significantly with increasing concentrations of both FIB concentrations. If FIB concentrations followed the pattern described by the first-flush hypothesis, correlations between short term measures of AP should reflect rapid increases in FIB concentrations. Instead, the results suggest that there are important long-term relationships and latency effects between precipitation onset and increasing FIB concentrations. This may also explain the relatively weak and inconsistent correlations between streamflow and FIB concentrations. If concentrations increase gradually, they may reach their highest levels well after peak streamflow, weakening the relationship between the two parameters.

Figure 5: Correlations of log-transformed FIB concentrations and water temperature.
***Spearman's rank correlations significant at $p < 0.001$.**



Both FC and EC log-transformed concentrations were moderately but significantly correlated with water temperature (Figure 5).

Land cover, Impervious Surfaces and FIB Concentrations

Land Cover Change, 1999-2005

Comparisons of land cover data from the 2001 and 2006 NLCD indicate rapid changes in land use both within individual creek watersheds and across the entire study area (Table 11). While percent changes on the scale of individual watersheds varied considerably, the overall pattern is of net increases in development, agricultural use and impervious surfaces and a net decrease in forested lands. The smallest increases in percent development and imperviousness occurred in watersheds that were already highly developed in 1999 (TFWP, SC) or where local land use policy or regulations restrict new building (CBC, MCWC).

Table 11: Land cover and imperviousness of individual creek watersheds in Oct. 1999, Oct. 2005 and percent change.

Creek	Area (ha)	Land cover classification											
		Developed			Agricultural			Forested			Imperviousness		
		1999	2005	% change	1999	2005	% change	1999	2005	% change	1999	2005	% change
MCWC	2197.5	5.27	5.31	0.9	22.04	22.55	2.3	71.92	71.50	-0.6	0.46	0.46	0.0
MWC	231.1	83.51	85.71	2.6	0.00	0.00	0.0	16.49	14.29	-13.4	33.33	34.01	2.0
MCCH	10420.3	18.23	18.29	0.4	14.32	14.87	3.8	66.28	65.73	-0.8	3.98	4.01	0.9
LCPGC	4929.5	54.05	55.15	2.0	5.14	4.59	-10.7	39.81	39.27	-1.3	9.92	10.24	3.2
MC1726	12008.8	19.07	19.16	0.5	13.47	14.08	4.6	64.86	64.16	-1.1	4.07	4.13	1.4
NHCB	19733.6	39.32	40.41	2.8	7.85	8.30	5.7	47.28	45.79	-3.2	8.33	8.78	5.4
NECG	5463.5	55.06	57.10	3.7	4.84	4.67	-3.4	35.59	33.85	-4.9	13.67	14.43	5.6
NECLG	779.1	61.54	67.15	9.1	2.68	2.26	-15.8	34.86	29.90	-14.2	13.04	14.95	14.6
TFWP	3839.8	84.40	85.35	1.1	0.78	0.76	-2.6	10.68	9.79	-8.3	17.75	18.25	2.8
TFHHP	151.0	99.31	99.31	0.0	0.00	0.00	0.0	0.69	0.69	0.0	17.14	17.14	0.0
SC	1224.4	78.52	78.52	0.0	0.94	0.94	0.0	20.35	20.35	0.0	21.58	21.90	1.5
MUD	1383.7	33.07	34.55	4.5	8.20	10.89	32.9	55.91	51.80	-7.4	4.72	4.97	5.4
NHCE	8165.4	7.73	7.97	3.1	13.58	14.49	6.7	77.14	76.00	-1.5	1.01	1.08	6.5
NHCTF	5846.5	8.00	8.33	4.2	15.57	16.88	8.4	74.41	72.79	-2.2	1.21	1.30	7.6
CBC	141.8	11.76	11.76	0.0	9.97	9.97	0.0	76.98	76.98	0.0	3.61	3.61	0.0
Total	42135.4	37.31	38.24	2.5	8.74	9.04	3.4	49.90	48.71	-2.4	7.99	8.36	4.6

No watershed decreased in either developed lands or impervious surfaces. Forest land cover decreased in 12 of the 15 watersheds and across the entire study area. The trend of rapidly occurring land cover changes does not conflict with other data, such as economic indicators and census data that also reflect sustained local patterns of recent growth.

Correlations of Land Cover, Impervious Surfaces and FIB Concentrations

Correlations of EC and FC concentrations with land cover measures and impervious surface coverage followed the same pattern during both dry-weather and storm events (Table 12). FIB concentrations were positively correlated with measurements of individual creek watershed development and impervious surfaces.

Table 12: Spearman's rank-order correlations (R^2) of log-transformed FIB concentrations, land cover measures and impervious surface (IS) coverage during dry-weather (DW) and storm events.

	% Agricultural		% Forested		% Developed		% IS	
	<i>p</i>	ρ (R^2)	<i>p</i>	ρ (R^2)	<i>p</i>	ρ (R^2)	<i>p</i>	ρ (R^2)
FC DW	5.9×10^{-5}	-0.229 (0.052)	3.5×10^{-5}	-0.236 (0.056)	2.0×10^{-5}	0.243 (0.06)	1.6×10^{-4}	0.216 (0.05)
FC Storm	0.06	-0.163 (0.027)	0.06	-0.165 (0.027)	0.04	0.178 (0.03)	0.045	0.173 (0.03)
EC DW	5.3×10^{-6}	-0.259 (0.067)	3.08×10^{-6}	-0.265 (0.070)	1.14×10^{-6}	0.276 (0.076)	1.85×10^{-5}	0.244 (0.060)
EC Storm	0.06	-0.161 (0.026)	0.07	-0.154 (0.024)	0.047	0.171 (0.029)	0.07	0.159 (0.025)

Conversely, FIB concentrations were negatively correlated with measurements of watershed agricultural and forested land cover. While all dry-weather correlations were statistically significant at $p < 0.001$, Spearman's rank correlation coefficients were small. This is likely the result of high variation in FIB concentrations at all creeks. Many of the storm correlations were not statistically significant at $p < 0.05$, likely the result of fewer samples and wider variation in FIB concentrations during storm events (Table 7).

Correlations of Land Cover, Impervious Surfaces and Total Loads Normalized for Watershed Area

Correlations of watershed area normalized FIB total loads, land cover measures and impervious surface coverage were more pronounced than corresponding FIB concentration correlations (Table 13). The resulting correlations had both greater strength and improved statistical significance. Storm loads of both FIB were more highly correlated with all measures of land cover and impervious surface coverage than dry-weather loads.

Table 13: Spearman's rank-order correlations of log-transformed watershed area normalized FIB total loads, land cover measures and impervious surface (IS) coverage during dry-weather (DW) and storm events.

	% Agricultural		% Forested		% Developed		% IS	
	<i>p</i>	rho (R ²)						
FC DW	2.0 x 10 ⁻⁶	-0.403 (0.162)	2.3 x 10 ⁻³	-0.266 (0.070)	3.3 x 10 ⁻⁶	0.395 (0.156)	4.1 x 10 ⁻⁶	0.391 (0.153)
FC Storm	0.026	-0.484 (0.234)	0.044	-0.444 (0.197)	0.026	0.484 (0.234)	0.025	0.488 (0.238)
EC DW	4.1 x 10 ⁻⁷	-0.427 (0.182)	5.9 x 10 ⁻⁴	-0.297 (0.088)	6.1 x 10 ⁻⁷	0.421 (0.177)	1.1 x 10 ⁻⁶	0.412 (0.170)
EC Storm	0.025	-0.488 (0.238)	0.036	-0.460 (0.238)	0.025	0.488 (0.238)	0.024	0.492 (0.242)

Development Intensity and Watershed Area

FIB concentrations varied by sample type and development intensity class (Table 14).

Table 14: Summary statistics of FIB concentrations (CFU/100 ml) by development intensity class and sample type

		Development intensity class			
		Low n = 141	Intermediate n = 151	High n = 144	
Sample Type	DW FC n = 301	Mean Std dev	396.50 785.61	556.77 1,208.97	845.23 1,493.75
	Storm FC n = 135	Mean Std dev	7,348.75 18,818.83	3,295.35 7,075.25	5,159.43 9,127.57
	DW EC n = 301	Mean Std dev	257.06 643.23	348.78 935.84	502.72 926.53
	Storm EC n = 135	Mean Std dev	900.87 1,783.11	514.73 765.79	719.47 907.36

During dry-weather, mean concentrations of both FC and EC clearly increased across development intensity classes. In the most developed watersheds both FIB concentrations were about twice those in the least developed watersheds. Mean storm concentrations of both FC and EC deviated from this pattern and had far greater variability. However; log-transformed median storm concentrations

were consistently greater than corresponding dry-weather measurements and increased with development intensity (Figure 6).

Another pattern emerged when samples were divided by watershed area (Table 15).

Table 15: Summary statistics of FIB concentrations (CFU/100 ml) by watershed area and sample type

		Watershed area category			
		Small n = 136	Medium n = 150	Large n = 150	
Sample Type	DW FC n = 301	Mean	887	586	366
		Std dev	1,555	1,211	743
	Storm FC n = 135	Mean	4,782	3,417	7,604
		Std dev	9,051	6,618	18,997
	DW EC n = 301	Mean	510	371	241
		Std dev	942	865	741
	Storm EC n = 135	Mean	700	700	735
		Std dev	850	1,061	1,678

During dry-weather, mean concentrations of both FC and EC from the smallest sized watersheds were 2-3 times greater than those from the largest ones. However, mean storm concentrations again deviated from this pattern.

Figure 6: Tukey box plots divided by development intensity (DI) class and sample type: FC (left) and EC (right).

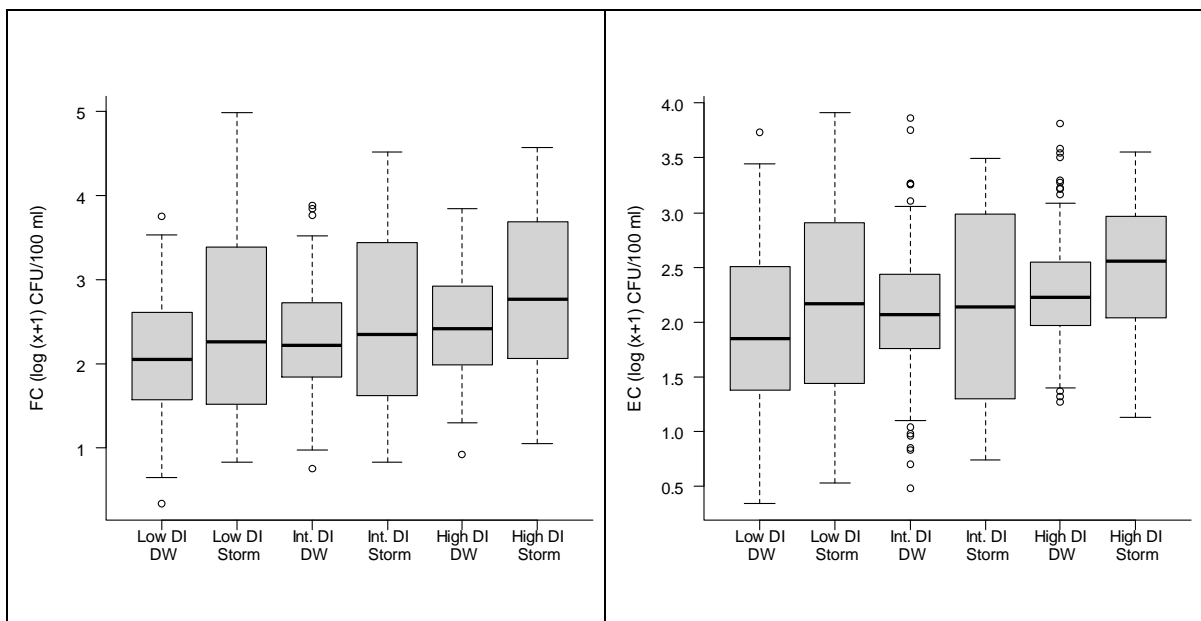
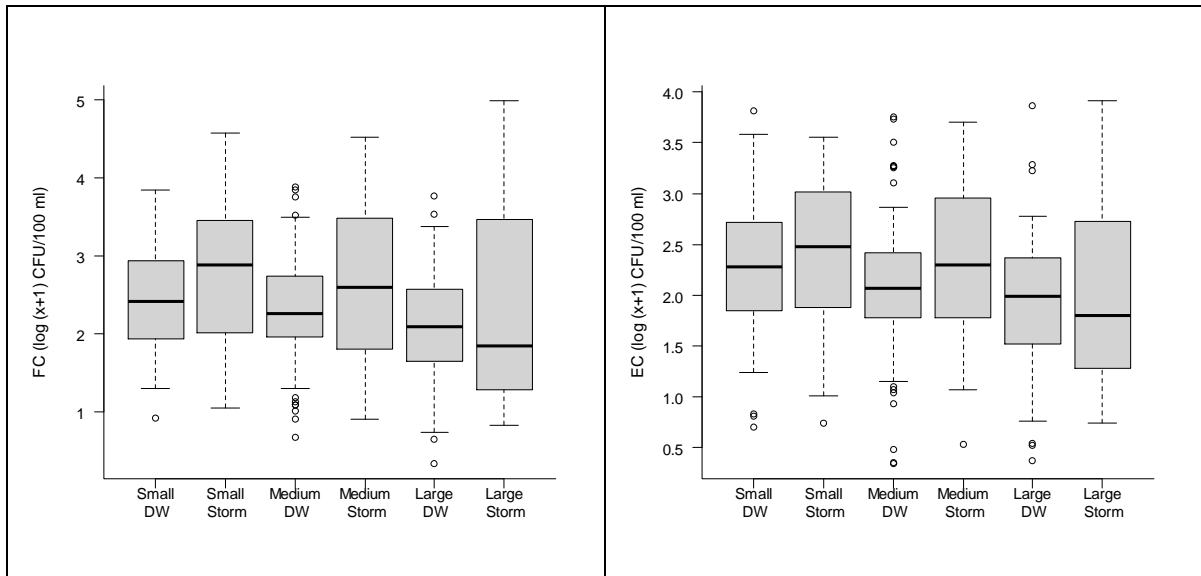


Figure 7: Tukey box plots divided by watershed area and sample type: FC (left) and EC (right).



The mean storm FC concentration in large watersheds was 1.5-2 times greater than either small or medium watersheds, while EC mean storm concentrations were remarkably consistent, regardless of watershed size. Median log-transformed concentrations mirrored these patterns (Figure 7).

3-factor ANOVA

For all FIB parameters, 3-factor analyses of variance were used to determine the significance of relationships between log-transformed concentrations, sample type, development intensity and watershed area (Table 16). Both sample type and development intensity were shown to have significant main effects on all FIB concentrations. Watershed area did not have a significant main effect on any of the FIB parameters. Also, there were no significant interaction effects between any of the factors on FC or EC concentrations. This can be interpreted to mean that all factor effects were uniform across all other factor levels. For all parameters, upstream watersheds having low (0.5 to 4.0%) and intermediate (4.1 to 14%) levels of imperviousness did not differ significantly.

Table 16: Results of 3-factor ANOVAs and pair-wise comparisons performed on log-transformed FIB concentrations.

Parameter	Factor			Pair wise comparisons	
	Sample type (Storm vs. DW) <i>p</i>	Development intensity <i>p</i>	Watershed area <i>p</i>	Sample type	Development intensity
EC	0.02	8.54×10^{-5}	0.09	DW ^a Storm ^b	Low ^a Int ^a High ^b
FC	2.98×10^{-5}	5.88×10^{-4}	0.12	DW ^a Storm ^b	Low ^a Int ^a High ^b
EC (EMC)	0.015	9.95×10^{-5}	0.37	DW ^a Storm ^b	Low ^a Int ^{a,b} High ^b
FC (EMC)	3.22×10^{-3}	8.71×10^{-3}	0.89	DW ^a Storm ^b	Low ^a Int ^a High ^b

Tukey pair wise comparisons were performed on significant factors. Factor levels with same superscripts were not significantly different at $p < 0.05$.

DW= dry-weather; Int = Intermediate

However, FIB concentrations were significantly greater in watersheds assigned to the high intensity development class (15 to 34%). While these results do not necessarily support a specific watershed imperviousness threshold, they do indicate that watersheds with highest levels of imperviousness have significantly greater FIB concentrations.

Conclusions

In the Jordan Lake watershed microbial NPS pollution was significantly influenced by antecedent precipitation and the intensity of watershed development. On average, watersheds with the highest measures of urban land use and impervious surfaces had significantly greater FIB concentrations during both dry-weather and storm events. However, longer duration measures of antecedent precipitation were more strongly correlated with FIB concentration than any measure of watershed land use. While the idea of simple watershed development or imperviousness thresholds is attractive, these results do not support any generalization about land use and microbial NPS pollution. For instance, intra-storm loading was consistently uniform over the course of all storms, regardless of watershed imperviousness. While the first-flush hypothesis may adequately describe

the loading pattern of other important NPS pollutants, our results concur with other studies of microbial NPS pollution that have failed to observe this phenomenon.

These results should improve water quality managers understanding of loading patterns in the Jordan Lake watershed. An important implication of these findings is that BMPs designed to mitigate microbial pollutant loads during the initial phase of stormwater runoff may function less efficiently than expected if loads are evenly distributed. Additionally, because storm event FIB concentrations are significantly greater than dry-weather samples and also demonstrate considerable intra-storm variation, single-sample monitoring efforts may inadequately describe stormwater impacts.

A central question raised by these results is whether traditional bacterial indicators accurately reflect microbial contamination. If environmental reservoirs of bacteria contribute to surface water FIB concentrations, conclusions about the magnitude, timing and distribution of microbial contamination resulting from stormwater may be inaccurate. Future research of stormwater loading should include indicators with no known or suspected environmental reservoirs. Additionally, the environmental persistence and potential replication of traditional FIB in North Carolina surface waters should be investigated.

Appendix A: Supplementary Tables and Figures

Figure 8: Storm event 1 hydrographs at all gauged creeks.

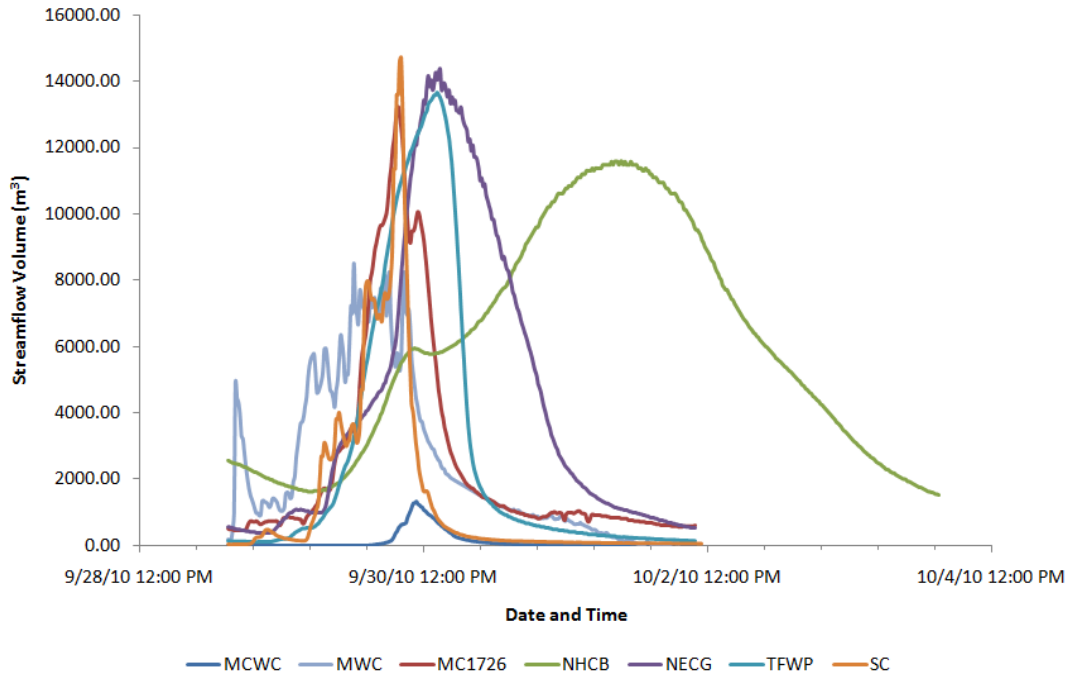


Figure 9: Storm event 2 hydrographs at all gauged creeks.

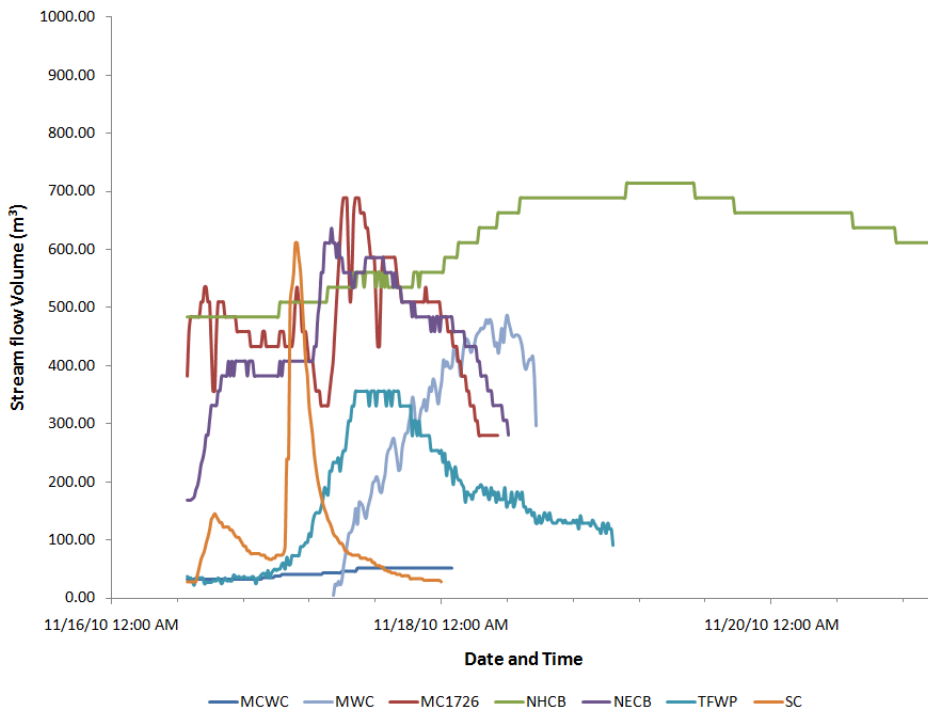


Figure 10: Storm event 3 hydrographs at all gauged creeks.

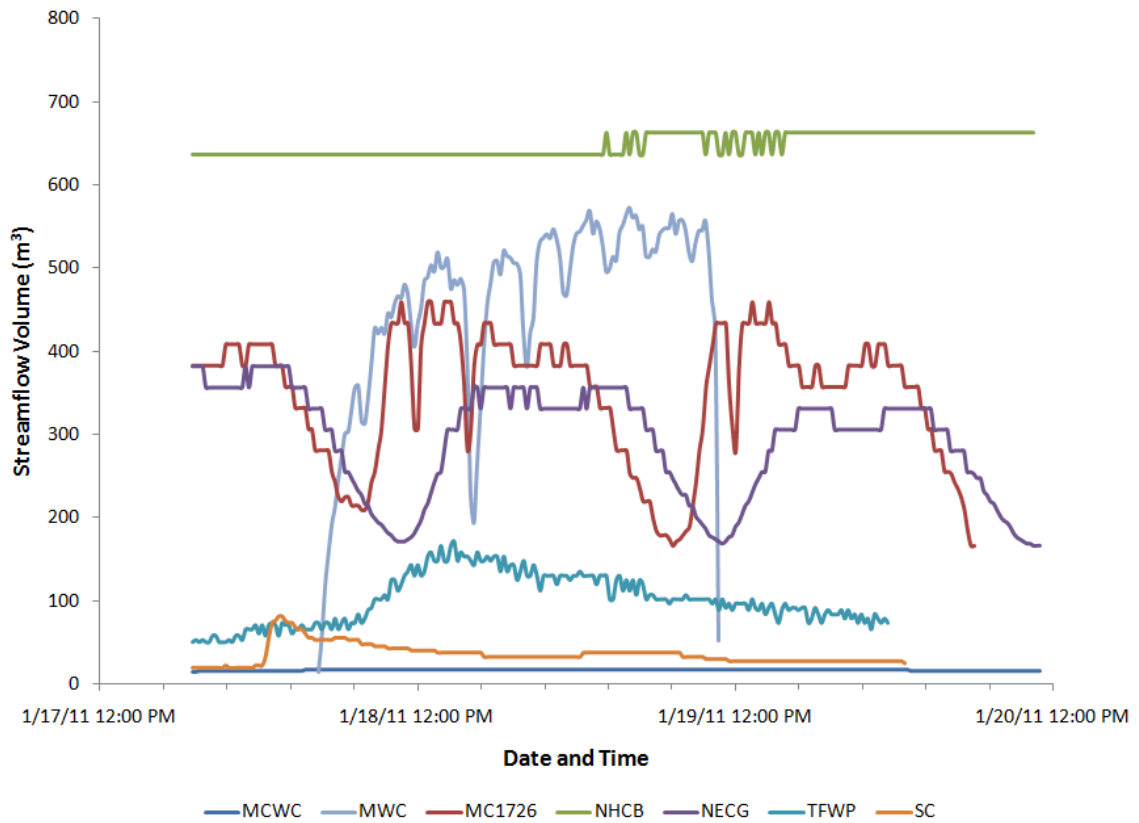


Table 17: Storm event loading, Morgan Creek at White Cross, NC (MCWC).

Storm Event	FC (CFU/storm)	DW days	EC (CFU/storm)	DW days	FC EMC (CFU/100 ml)	Times greater	EC EMC (CFU/100 ml)	Times greater
Storm 1	4.27×10^{12}	461.1	1.72×10^{12}	309.2	10700	41.7	4323	30.3
Storm 2	1.34×10^{10}	1.4	8.03×10^9	1.4	203	0.8	122	0.9
Storm 3	2.14×10^9	0.2	2.08×10^9	0.4	37	0.1	36	0.3
Storm Average	1.43×10^{12}	154.6	5.78×10^{11}	103.6	3647	14.2	1494	10.4

Table 18: Storm event loading, Meeting of the Waters Creek (MWC).

Storm Event	FC (CFU/storm)	DW days	EC (CFU/storm)	DW days	FC EMC (CFU/100 ml)	Times greater	EC EMC (CFU/100 ml)	Times greater
Storm 1	7.24×10^{13}	479.3	8.97×10^{12}	91.3	10305	26.7	1276	5.4
Storm 2	9.72×10^{11}	6.4	3.87×10^{10}	0.4	2572	6.7	103	0.4
Storm 3	1.62×10^{11}	1.1	1.29×10^{11}	1.3	290	0.8	232	1.0
Storm Average	2.45×10^{13}	162.3	3.05×10^{12}	31.1	4389	11.4	537	2.3

Table 19: Storm event loading, Morgan Creek at NC-1726 (MC1726).

Storm Event	FC (CFU/storm)	DW days	EC (CFU/storm)	DW days	FC EMC (CFU/100 ml)	Times greater	EC EMC (CFU/100 ml)	Times greater
Storm 1	3.895×10^{13}	193.3	1.132×10^{13}	63.2	4882	8.4	1418.20	2.7
Storm 2	1.26×10^{11}	0.6	6.02×10^{10}	0.3	121	0.2	57.67	0.1
Storm 3	4.26×10^{10}	0.2	6.06×10^{10}	0.3	52	0.1	73.67	0.1
Storm Average	1.30×10^{13}	64.4	3.81×10^{12}	21.3	1685	2.9	517	1.0

Table 20: Storm event loading, New Hope Creek at Blands (NHCB).

Storm Event	FC (CFU/storm)	DW days	EC (CFU/storm)	DW days	FC EMC (CFU/100 ml)	Times greater	EC EMC (CFU/100 ml)	Times greater
Storm 1	5.16×10^{14}	1146.5	2.66×10^{13}	69.8	18134	62	935	4.5
Storm 2	4.32×10^{10}	0.1	6.68×10^{10}	0.2	14	0.1	22	0.1
Storm 3	1.30×10^{10}	0.0	1.19×10^{10}	0.0	8	0.0	8	0.0
Storm Average	1.72×10^{14}	382.2	8.90×10^{12}	23.4	6052	20.6	322	1.5

Table 21: Storm event loading, Northeast Creek at Genlee (NECG).

Storm Event	FC (CFU/storm)	DW days	EC (CFU/storm)	DW days	FC EMC (CFU/100 ml)	Times greater	EC EMC (CFU/100 ml)	Times greater
Storm 1	6.13×10^{13}	474.1	1.42×10^{13}	260.0	43634	16.0	1011	8.0
Storm 2	1.48×10^{11}	1.1	1.35×10^{11}	2.5	178	0.7	163	1.3
Storm 3	2.49×10^{10}	0.2	2.93×10^{10}	0.5	33	0.1	39	0.3
Storm Average	2.05×10^{13}	158.9	4.79×10^{12}	87.7	1525	5.6	404	3.2

Table 22: Storm event loading, Third Fork NHC at Woodcroft Parkway (TFWP).

Storm Event	FC (CFU/storm)	DW days	EC (CFU/storm)	DW days	FC EMC (CFU/100 ml)	Times greater	EC EMC (CFU/100 ml)	Times greater
Storm 1	5.73×10^{13}	944.7	2.29×10^{13}	559.7	6438	12.3	2579	6.9
Storm 2	2.14×10^{11}	3.5	1.33×10^{11}	3.3	520	1.0	323	0.9
Storm 3	1.07×10^{11}	1.8	1.06×10^{11}	2.6	361	0.7	359	1.0
Storm Average	1.92×10^{13}	324.9	7.73×10^{12}	204.5	2439	4.6	1087	2.9

Table 23: Storm event loading, Sandy Creek at Cornwallis Rd (SC).

Storm Event	FC (CFU/storm)	DW days	EC (CFU/storm)	DW days	FC EMC (CFU/100 ml)	Times greater	EC EMC (CFU/100 ml)	Times greater
Storm 1	2.18×10^{13}	631.7	7.53×10^{12}	613.4	4797	5.0	1657	4.7
Storm 2	1.01×10^{12}	29.3	3.14×10^{11}	25.6	4656	4.9	1448	4.1
Storm 3	1.73×10^{10}	0.5	1.74×10^{10}	1.4	219	0.2	222	0.6
Storm Average	7.61×10^{12}	238.1	2.62×10^{12}	213.0	3224	3.4	1109	3.2

Table 24: Summary of measured parameters during dry-weather (DW), storm events and combined, all creek sites.

	Temp. (°C)		pH		Diss. O ² (ppm)		Turbidity (NTU)		TDS (ppm)		Conductivity (S/m)		Streamflow (m ³ /sec)	
	Mean	SD	Mean	SD	Mean	SD	Mean	SD	Mean	SD	Mean	SD	Mean	SD
DW	15.5	7.5	7.8	0.4	6.3	2.8	14.8	21.3	192.4	21.3	244.9	156.6	0.4	0.5
Storm	12.9	6.7	7.7	0.3	8.1	1.7	17.0	24.5	218.9	24.5	241.9	213.0	1.5	3.3
All	14.7	7.4	7.8	0.4	6.8	2.6	15.5	22.3	200.6	22.3	244.0	175.8	0.7	1.9

Figure 11: Seasonal variation in daily dry-weather FIB load at all gauged creek sites and all creek sites combined.

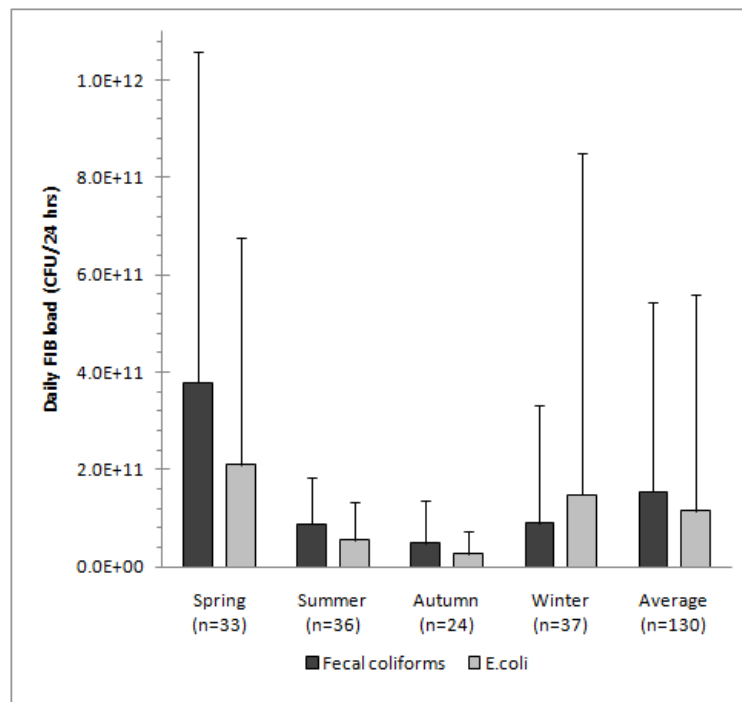


Figure 12: Storm event loading patterns at all gauged creek sites and all creek sites combined.

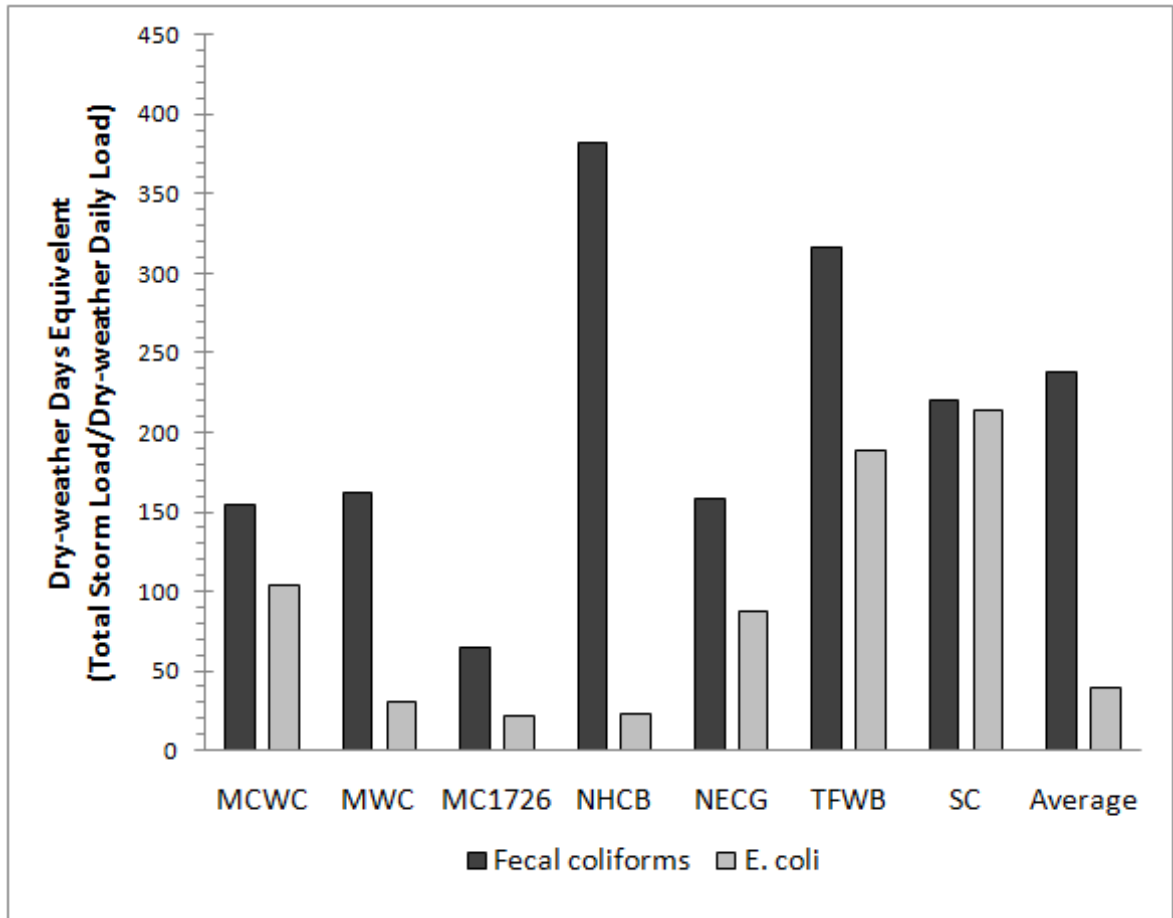


Figure 13: Individual FC M/V curves, Morgan Creek at NC-54 West (MCWC).

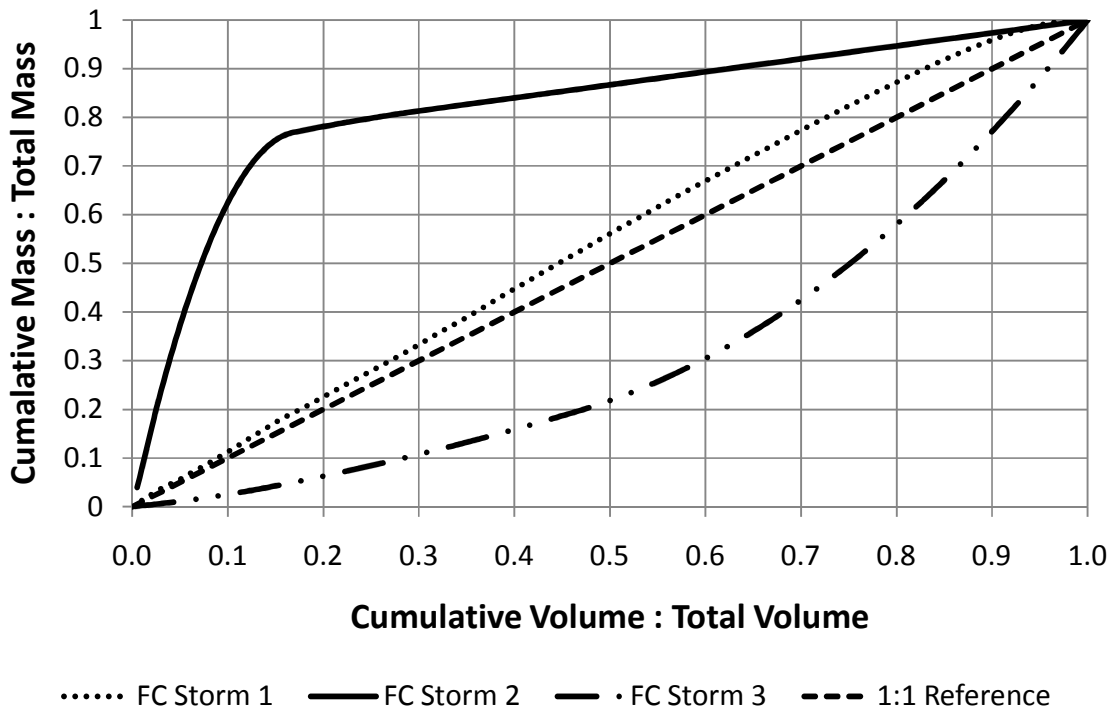


Figure 14: Individual EC M/V curves, Morgan Creek at NC-54 West (MCWC).

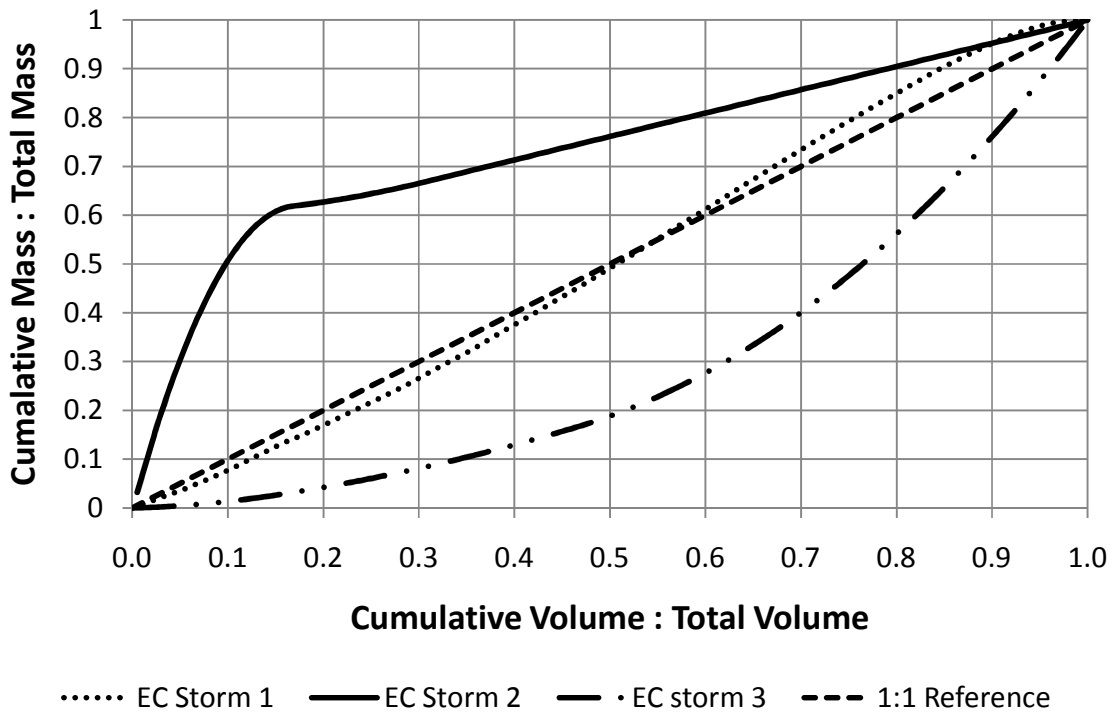


Figure 15: Individual FC M/V curves, Meeting of the Water Creek (MWC).

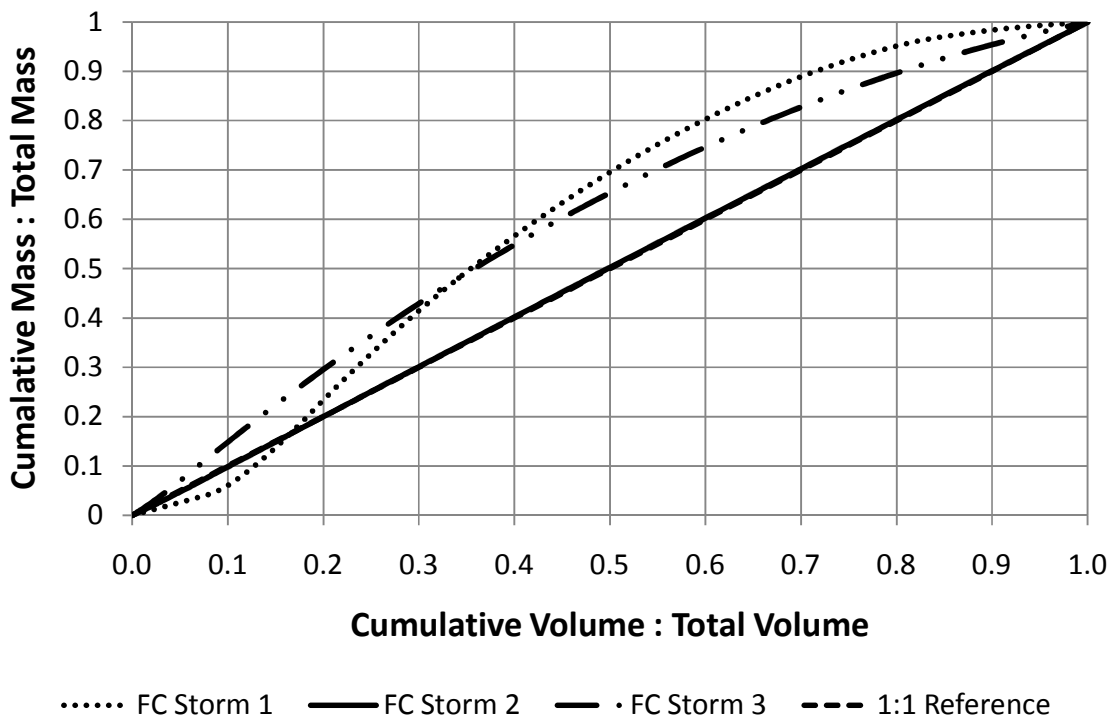


Figure 16: Individual EC M/V curves, Meeting of the Water Creek (MWC).

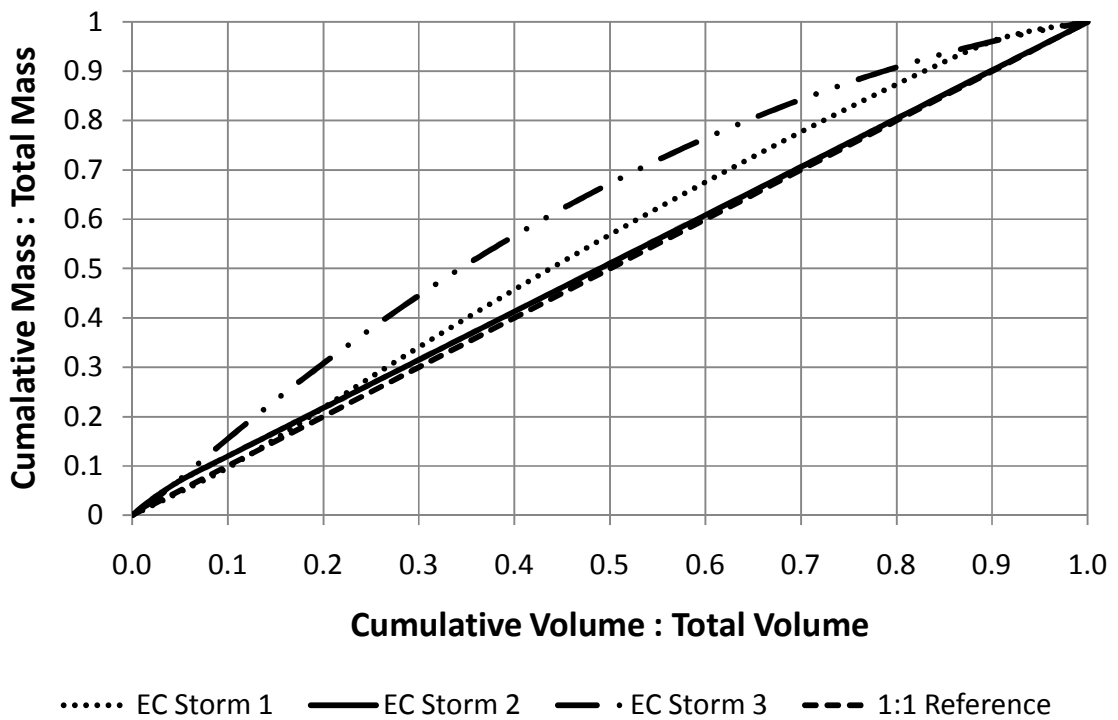


Figure 17: Individual FC M/V curves, Morgan Creek at NC-1726 (MC1726).

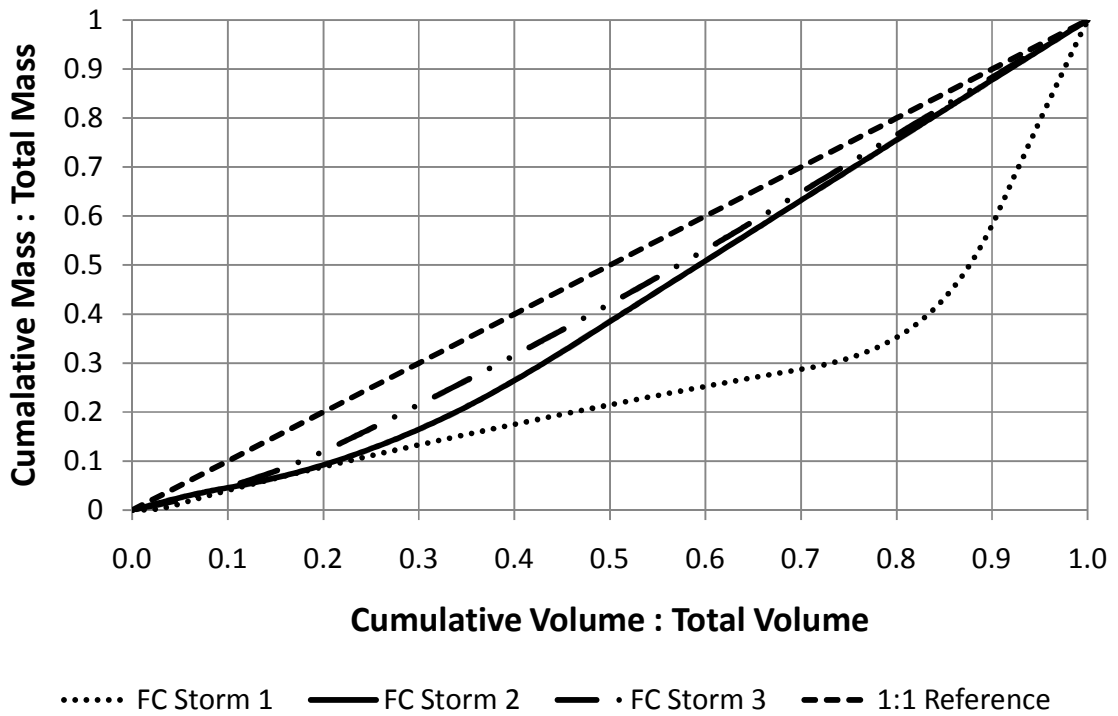


Figure 18: Individual EC M/V curves, Morgan Creek at NC-1726 (MC1726).

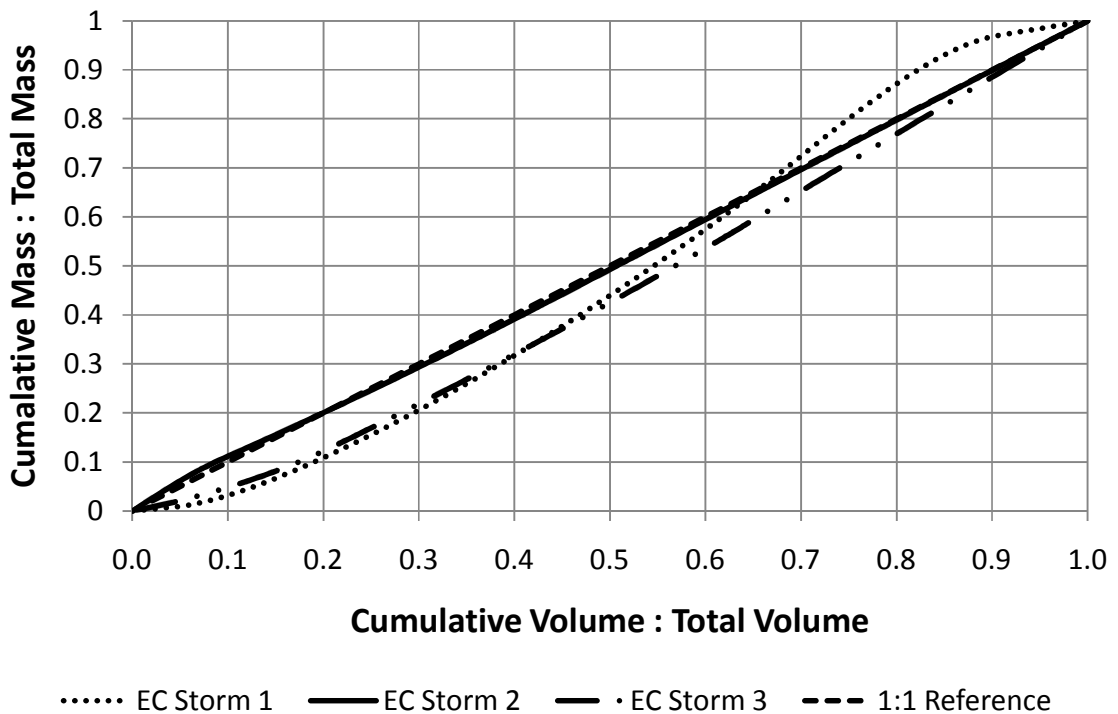


Figure 19: Individual FC M/V curves, New Hope Creek at Blands (NHCB).

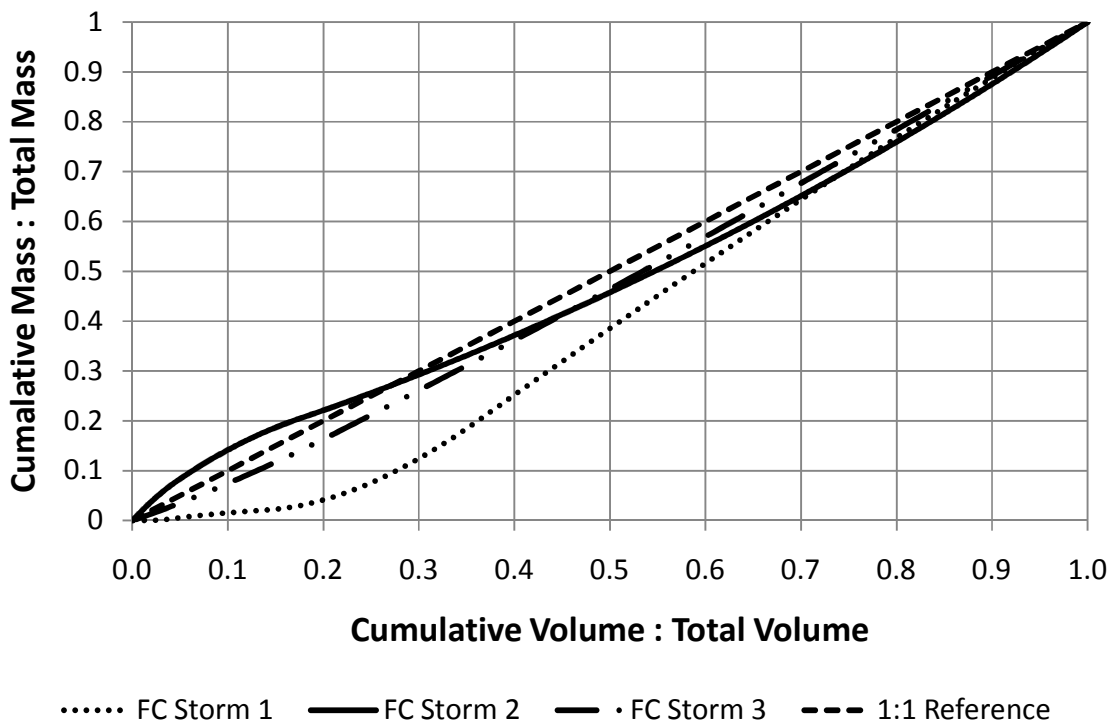


Figure 20: Individual EC M/V curves, New Hope Creek at Blands (NHCB).

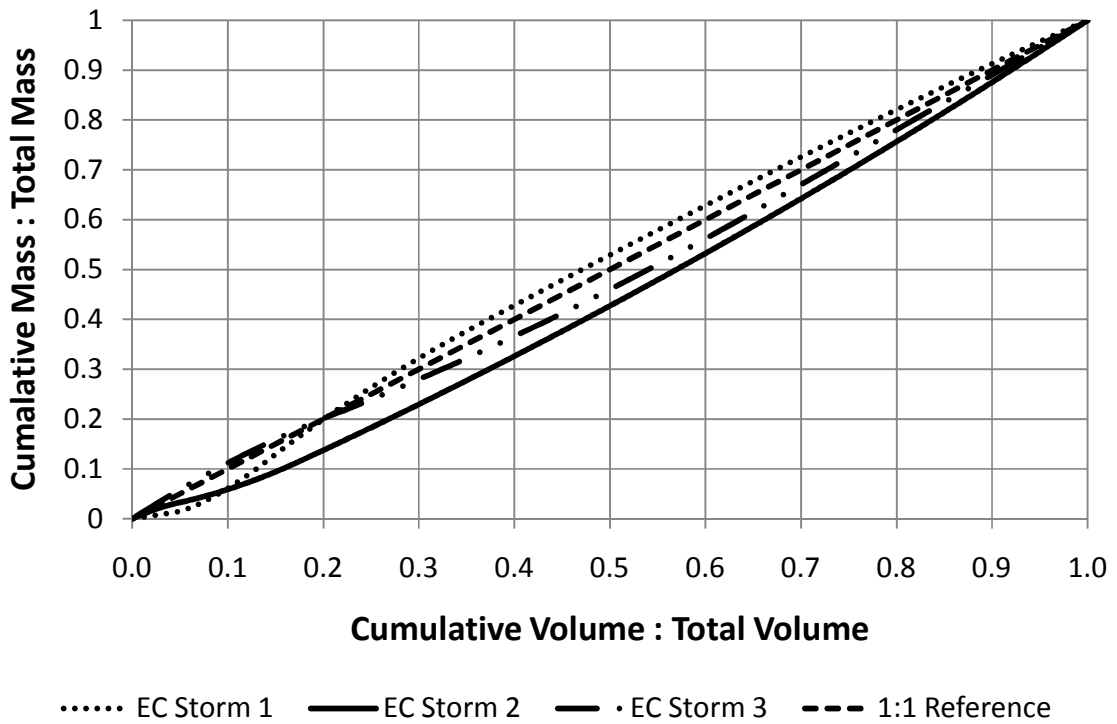


Figure 21: Individual FC M/V curves, Northeast Creek at Genlee (NECG).

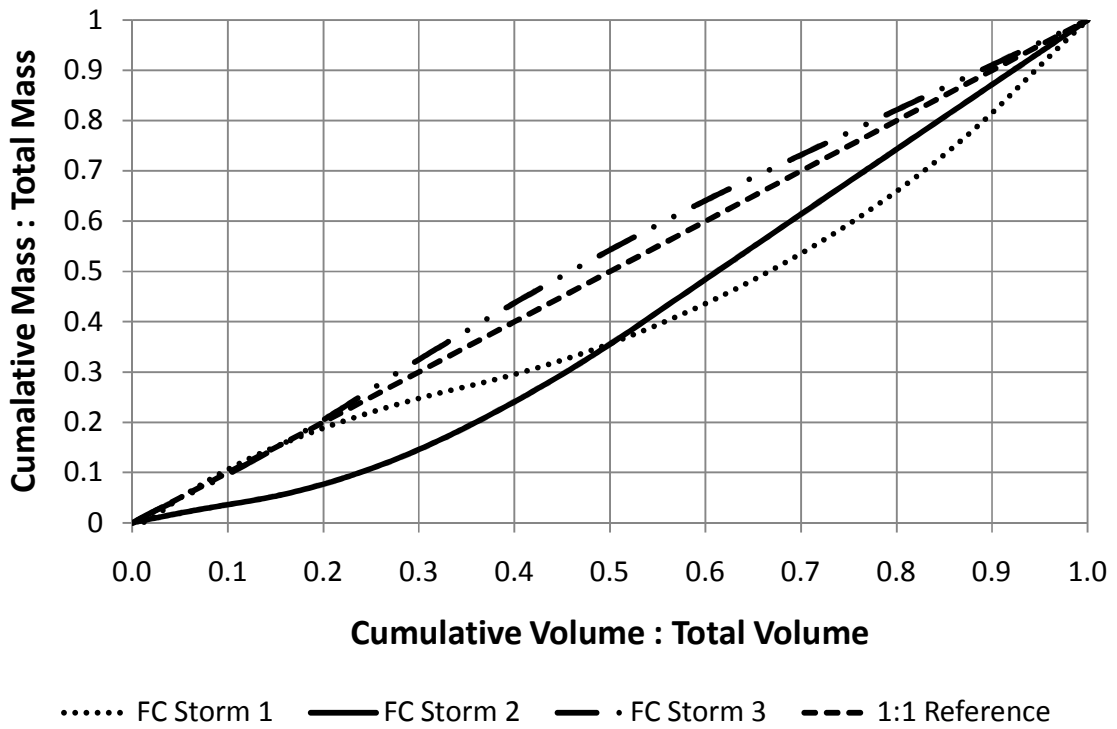


Figure 22: Individual EC M/V curves, Northeast Creek at Genlee (NECG).

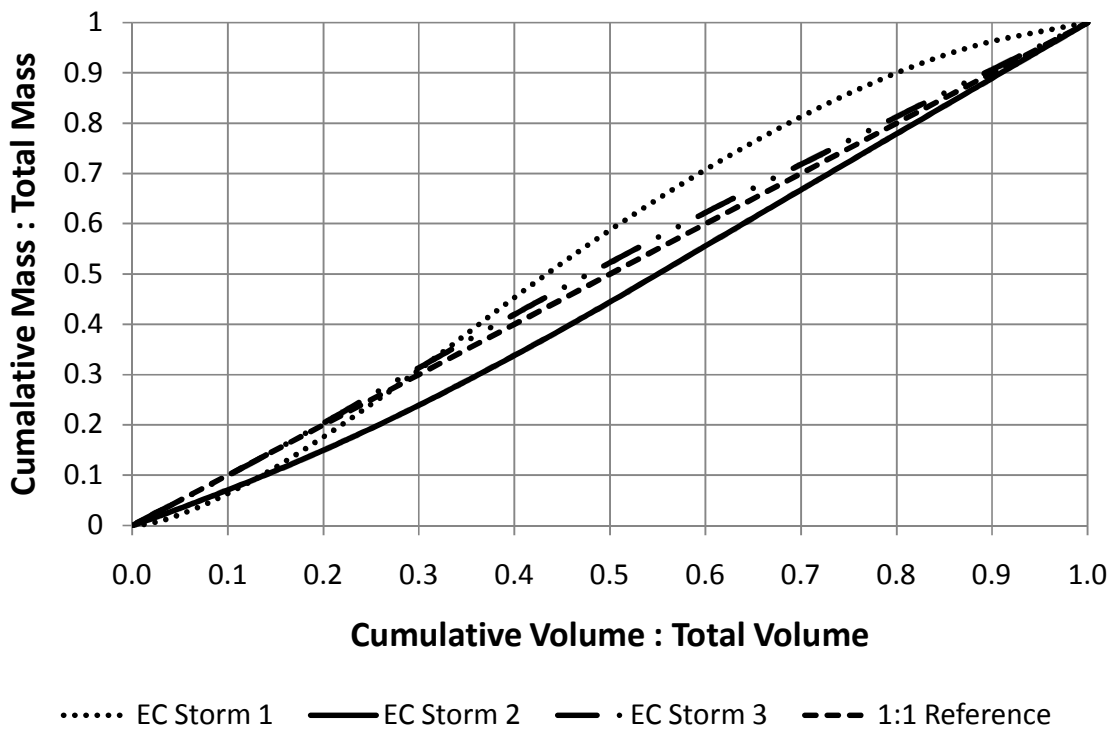


Figure 23: Individual FC M/V curves, Third Fork NHC at Woodcroft Parkway (TFWB).

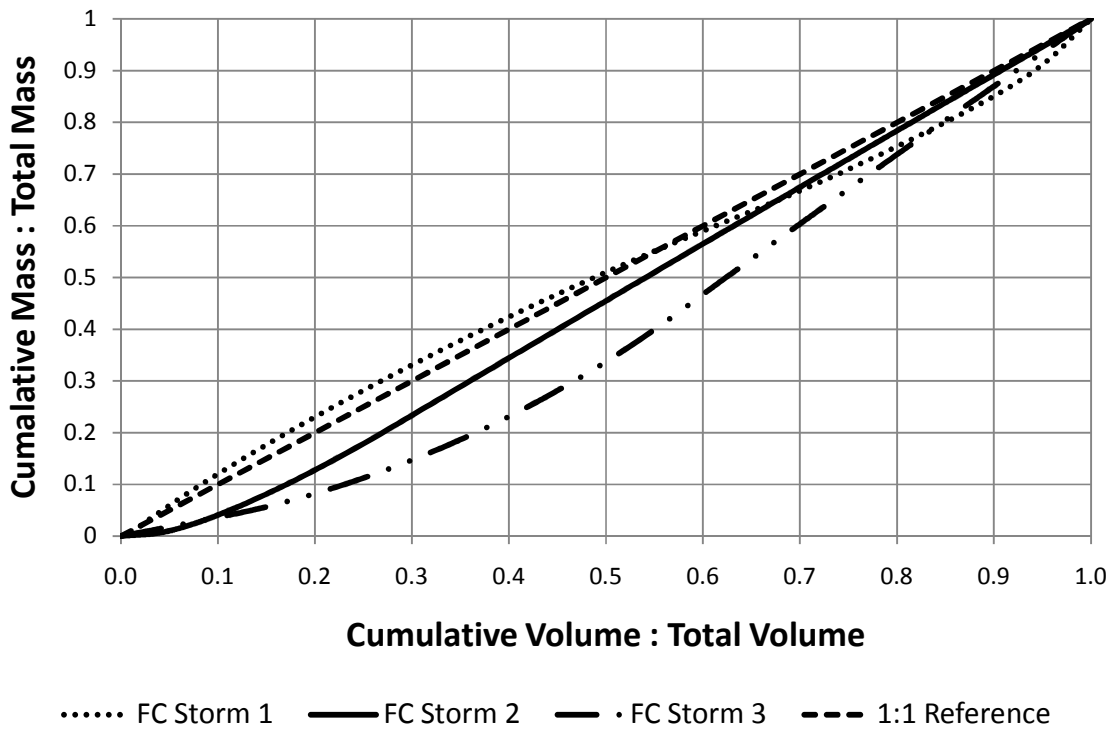


Figure 24: Individual EC M/V curves, Third Fork NHC at Woodcroft Parkway (TFWB).

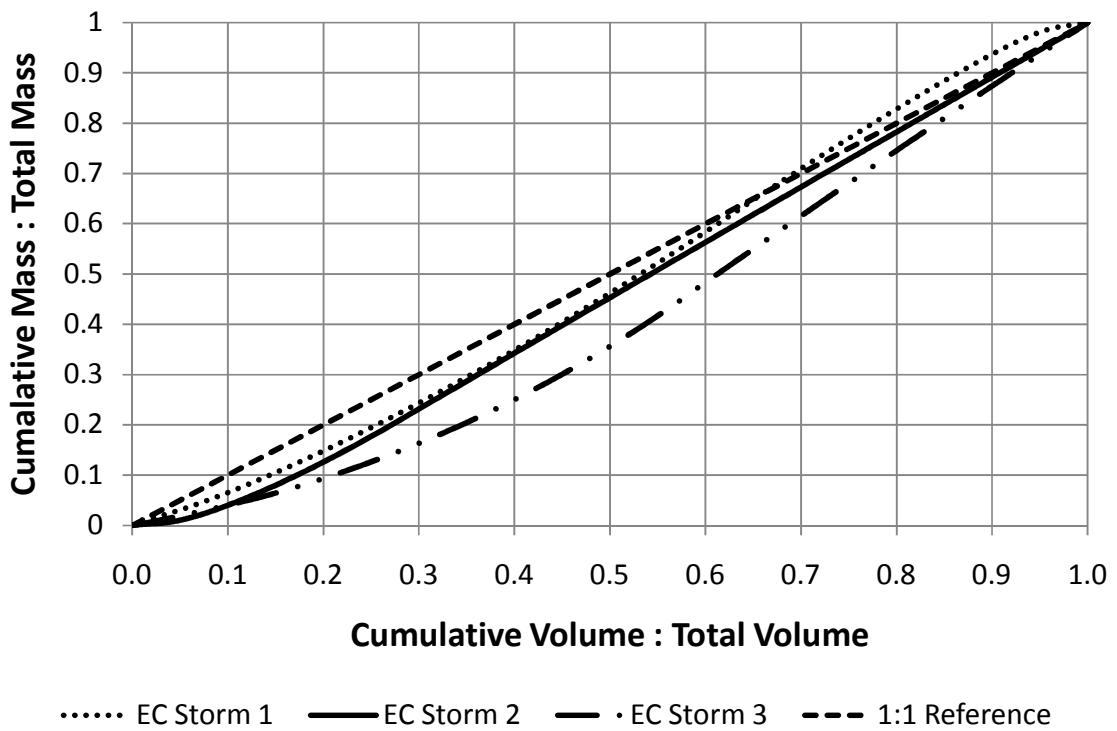


Figure 25: Individual FC M/V curves, Sandy Creek at Cornwallis Rd (SC).

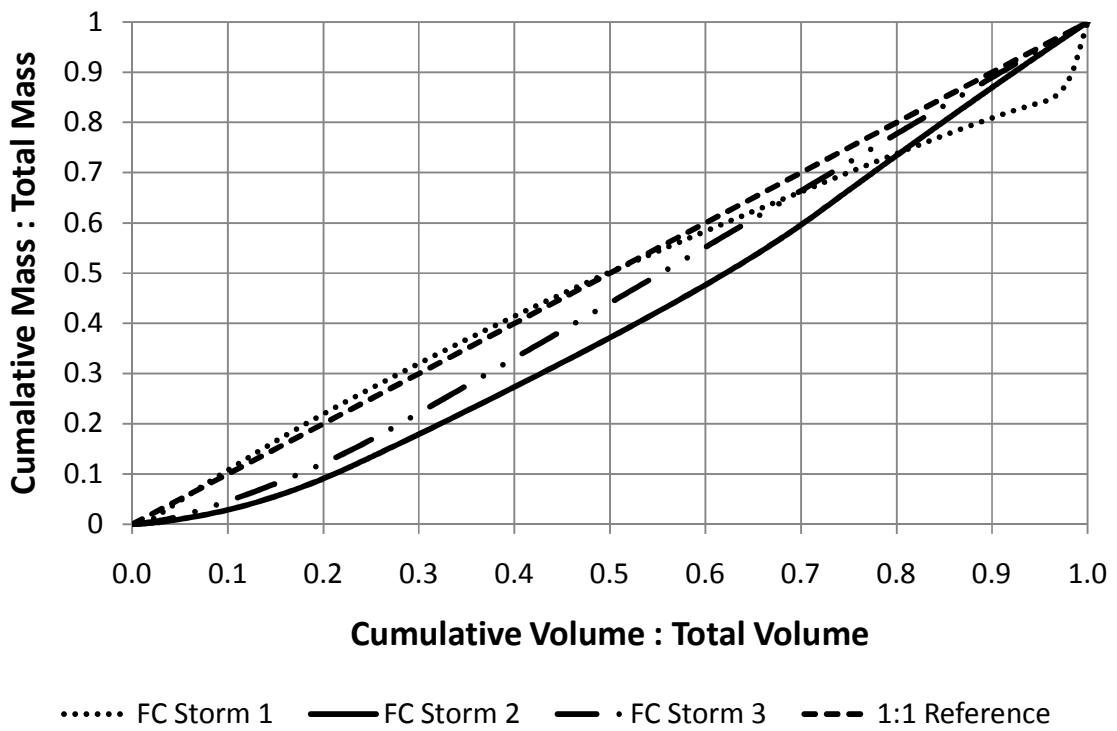


Figure 26: Individual EC M/V curves, Sandy Creek at Cornwallis Rd (SC).

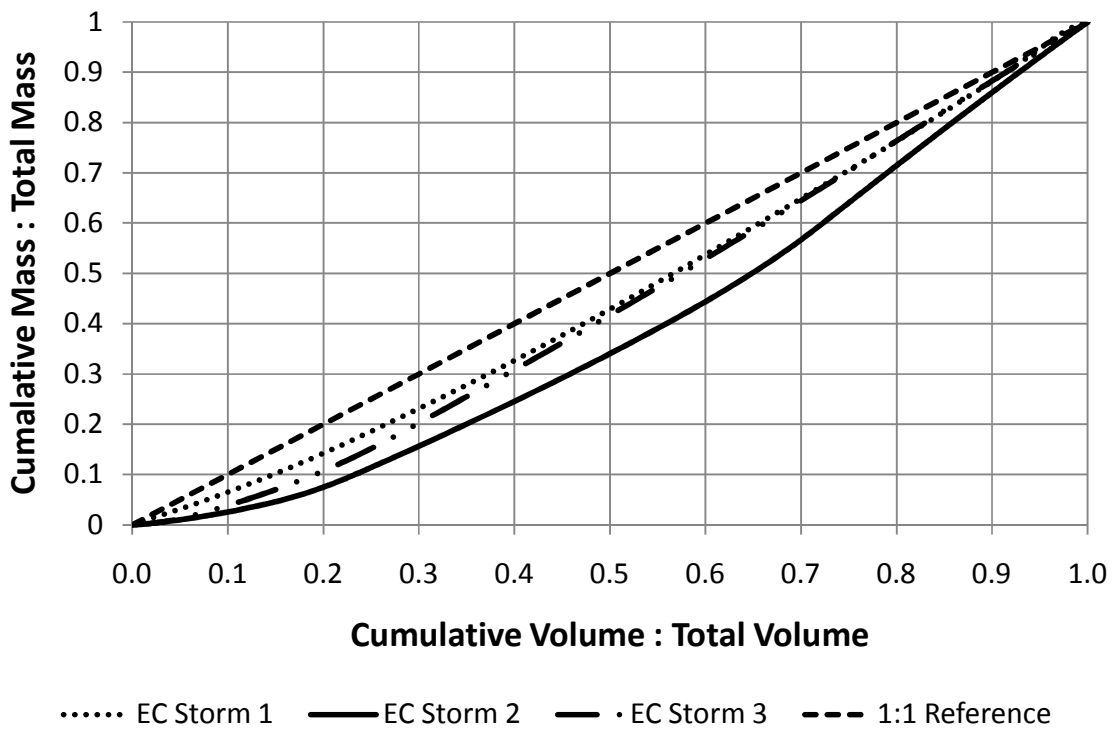


Figure 27: Detail of “bridge buddy” sample collection device being readied for use.



Figure 28: A field technician prepares to collect a sample by lowering the device into the creek below.



References

- APHA, 1998. Standard methods for the examination of water and wastewater. American Public Health Association, Washington, DC.
- Arnold, C., Gibbons, C.J., 1996. Impervious surface coverage: the emergence of a key environmental indicator. *Journal of the American Planning Association*. Vol. 62(2): 243-258.
- Baker, L. 1992. Introduction to nonpoint source pollution in the United States and prospects for wetland use. *Ecological Engineering*. Vol. 1, No. 1 (3): 1-26.
- Band, L. E., Tague, C. L., Groffman, P., Belt, K., 2001. Forest ecosystem processes at the watershed scale: hydrological and ecological controls of nitrogen export. *Hydrological Processes*. Vol. 15(10), 2013-2028.
- Barling, R. D., Moore. I. D., 1994. Role of buffer strips in management of waterway pollution: a review. *Environmental Management*. Vol. 18, No. 4 (7): 543-558.
- Bertrand-Krajewski, J., Chebbo G., Saget, A., 1998. Distribution of pollutant mass vs volume in stormwater discharges and the first flush phenomenon. *Water Research*. Vol. 32, No. 8 (8): 2341-2356.
- Bledsoe, B. P., Watson C. C., 2001. Effects of urbanization on channel instability. *Journal of the American Water Resources Association*. Vol. 37, No. 2 (4): 255-270.
- Booth, D., 1991. Urbanization and the natural drainage system—impacts, solutions and prognoses. *Northwest Environ. J*. Vol. 7(1): 93–118.
- Booth, D. B., Jackson, C. R., 1997. Urbanization of aquatic systems: degradation thresholds, stormwater detection, and the limits of mitigation. *Journal of the American Water Resources Association*. Vol. 33, No. 5 (10): 1077-1090.
- Brown, D. G., Johnson, K. M., Loveland, T. R., Theobald, D. M., 2005. Rural land-use trends in the conterminous United States, 1950–2000. *Ecological Applications* Vol. 15(6), 1851-1863.
- Byappanahalli, M., Fowler, M., Shively, D., Whitman, R., 2003. Ubiquity and persistence of *E. coli* in amid-western coastal stream. *Appl. Environ. Microbiol.* Vol. 69, 4549-4555.
- Carle, M.V., Halpin, P.N., Stow, C.A., 2005. Patterns of watershed urbanization and impacts on water quality. *Journal of the American Water Resources Association*. Vol. 41(3): 693-708.
- Carpenter, S. R., Caraco, N. F., Correll, D. L., Howarth, R. W., Sharpley, A. N., Smith. V. H., 1998. Nonpoint pollution of surface waters with phosphorus and nitrogen. *Ecological Applications*. Vol. 8, No. 3 (8).
- Craun, G. F., Calderon, R. L., Craun, M. F., 2005. Outbreaks associated with recreational water in the United States. *Int J Environ Health Res*. Vol. 15(4): 243-262.

- Curriero, F. C., Patz, J. A., Rose, J. B., Lele, S., (2001). The association between extreme precipitation and waterborne disease outbreaks in the United States, 1948-1994. *Am J Public Health*. Vol. 91(8): 1194-1199.
- Coulliette, A.D., Money, E. S., Serre, M. L., Noble, R. T., 2009. Space/time analysis of fecal pollution and rainfall in an eastern north carolina estuary. *Environmental Science & Technology*. Vol. 43(10), 3728-3735.
- Didonato, G. Stewart, J., Sanger, D., Robinson, B., Thompson, B., Holland, A., Vandolah, R., 2009. Effects of changing land use on the microbial water quality of tidal creeks. *Marine Pollution Bulletin*. Vol. 58(1): 97-106.
- Deletic, A., 1998. The first flush load of urban surface runoff. *Water Research*. Vol. 32, No. 8 (8): 2462-2470.
- Drayna, P., McLellan, S. L., Simpson, P., Li, S., Gorelick, M. H., 2010. Association between rainfall and pediatric emergency department visits for acute gastrointestinal illness. *Environmental Health Perspectives*. Vol. 118(10): 1439-1443.
- Edwards, D. R., Daniel, T. C., 1992. Environmental impacts of on-farm poultry waste disposal – a review. *Bioresource Technology*. Vol. 41(1), 9–33.
- Fujioka, R., Sian-Denton, C., Borja, M., Castro, J., Morphew, K., 1999. Soil: the environmental sources of *E. coli* and enterococci in Guam's streams. *J. Appl. Microbiol. Symp. Supplement*. Vol. 85: 83-89.
- Frenzel, S.A., Couvillion, C.S., 2002. Fecal-indicator bacteria in streams along a gradient of residential development. *Journal of the American Water Resources Association*. Vol. 33(1): 265-273.
- Galli, J., 1990. Thermal impacts associated with urbanization and stormwater management best management practices. *Metro. Wash. Counc. Gov., Maryland Dep. Environ. Washington, D.C.* 188 pp.
- Goonetilleke, A., Thomas, E., Ginn. S., Gilbert, D., 2004. Understanding the role of land use in urban stormwater quality management. *Journal of Environmental Management* Vol. 74, 31-42.
- Groffman, P. M., Law, N. L., Belt, K. T., Band, L. E., & Fisher, G. T. (2004). Nitrogen fluxes and retention in urban watershed ecosystems. *Ecosystems*. Vol. 7(4): 393-403.
- Hammer, D. 1992. Designing constructed wetlands systems to treat agricultural nonpoint source pollution. *Ecological Engineering*. Vol. 1, No. 1 (3): 49-82.
- Homer, C., Huang C., Yang, L., Wylie, B., Coan, M., 2004. Development of a 2001 National Landcover Database for the United States. *Photogrammetric Engineering and Remote Sensing*, Vol. 70, No. 7, July 2004, pp. 829-840.
- Homer, C., Dewitz, J., Fry, J., Coan, M., Hossain, N., Larson C., et al., 2007. Completion of the 2001 National Land Cover Database for the conterminous United States, *Photogrammetric Engineering and Remote Sensing*. Vol. 73 (4): 337–341.

- Hatt, B. E., Fletcher, T. D., Walsh, C. J., Taylor, S. L. (2004). The influence of urban density and drainage infrastructure on the concentrations and loads of pollutants in small streams. *Environmental Management*. Vol. 34(1).
- James, E., Joyce, M., 2004. Assessment and management of watershed microbial contaminants. *Critical Reviews in Environmental Science and Technology*. Vol. 34, No. 2 (3): 109-139.
- Jones, R., Clark. C., 1987. Impact of watershed urbanization on stream insect communities. *Am. Water Resour. Assoc. Water Resour. Bull.* Vol. 15(4)
- Karr, J. R., Dudley D. R., 1981. Ecological perspective on water quality goals. *Environmental Management* Vol. 5:55-68.
- Karr, J. R., Chu E. W., 2000. Sustaining living rivers. *Hydrobiologia*. Vol. 422-423, Number 0: 1-14.
- Kistemann, T., Classen, T., Koch, C., Dangendorf, F., Fischeider, R., Gebel, J., Vacata, V., et al., 2002. Microbial load of drinking water reservoir tributaries during extreme rainfall and runoff. *Applied and Environmental Microbiology*, Vol. 68(5), 2188-2197.
- Krometis, L., Characklis, G., Simmonsiii, O., Dilts, M., Likirdopulos, C., Sobsey, M., 2007. Intra-storm variability in microbial partitioning and microbial loading rates. *Water Research*. Vol. 41, No. 2 (1): 506-516.
- Lenat, D. R., 1984. Agriculture and stream water quality: a biological evaluation of erosion control practices. *Environmental Management*. Vol. 8, No. 4 (7): 333-343.
- Lee, J.H., Bang, K.W., Ketchum Jr., L.H., Choe, J.S., Yu, M.J., 2002. First flush analysis of urban storm runoff. *Science of the Total Environment*. Vol. 293, No. 1 (7): 163-175.
- Lee, H., Lau, S., Kayhanian, M., Stenstrom, M., 2004. Seasonal first flush phenomenon of urban stormwater discharges. *Water Research*. Vol. 38, No. 19 (11): 4153-4163.
- Li, L, Yin, C., He, Q., Kong, L., 2007. First flush of storm runoff pollution from an urban catchment in China. *Journal of Environmental Sciences*. Vol. 19, No. 3 (3): 295-299.
- Limburg, K., and R. Schimdt 1990. Patterns of fish spawning in Hudson River tributaries—response to an urban gradient? *Ecology*. Vol. 71(4): 1231–1245.
- Line, D. E., Wu, J., Arnold, J. A., Jennings, G. D., Rubin, A. R., 1997. Water quality of first flush runoff from 20 industrial sites. *Water Environment Research*. Vol. 69, No. 3: 305-310
- Mallin, M. A., Ensign S. H., McIver M. R., Shank G. C., Fowler, P. K., 2001. Demographic, landscape, and meteorological factors controlling the microbial pollution of coastal waters *Hydrobiologia*. Vol. 460, Numbers 1-3: 185-193.
- Mallin, M. A., Cahoon, L. B., 2003. Industrialized animal production—a major source of nutrient and microbial pollution to aquatic ecosystems. *Population & Environment*. Vol. 24, No. 5, 369-385.

- Mallin, M. A., Johnson, V. L., Ensign S. H., 2008. Comparative impacts of stormwater runoff on water quality of an urban, a suburban, and a rural stream. *Environmental Monitoring and Assessment*. Vol. 159, No. 1 (12): 475-491.
- Messner, M., Shaw, S., Regli, S., Rotert, K., Blank, V., Soller, J., 2006. An approach for developing a national estimate of waterborne disease due to drinking water and a national estimate model application. *Journal of Water and Health*. Vol. 4(Suppl 2): 201.
- Milesi, C., 2003. Assessing the impact of urban land development on net primary productivity in the southeastern United States. *Remote Sensing of Environment*. Vol. 86(3): 401-410.
- Nash, D., 2000. Tracing phosphorous transferred from grazing land to water. *Water Research*. Vol. 34, No. 7 (5): 1975-1985.
- National Research Council, 2008a. Urban stormwater management in the United States, Water Science Technology Board. "Integrating multiscale observations of U.S. waters." National Academies Press, 181p.
- National Research Council, 2008b. Committee on Integrated observations for hydrologic and related sciences, Water Science Technology Board. "Integrating multiscale observations of U.S. waters." National Academies Press, 513p.
- NCDENR, 2005. Basin wide assessment report: Cape Fear River Basin. North Carolina. URL: <http://h2o.enr.state.nc.us/basinwide/draftCPFApril2005.htm>.
- NSTC-SWAQ, 2007. *A Strategy for Federal Science and Technology to Support Water Availability and Quality in the United States*. Report of the National Science and Technology Council Committee on Environmental and Natural Resources. Subcommittee on Water Availability and Quality.
- R Development Core Team, 2010. R: a language and environment for statistical computing. R Foundation for Statistical Computing, Vienna, Austria. URL <http://www.R-project.org/>.
- Reynolds, K.A., Mena, K.D., Gerba, C.P., 2008. Risk of waterborne illness via drinking water in the United States. *Rev Environ Contam Toxicol*. Vol. 192: 117–158.
- Schueler TR., 1994. The importance of imperviousness. *Watershed Prot. Tech*. Vol. 1: 100–111
- Shields, C. A., Band, L. E., Law, N., Groffman, P. M., Kaushal, S. S., Savvas, K., Fisher, G. T., Belt, K. T., 2008. Streamflow distribution of non–point source nitrogen export from urban-rural catchments in the Chesapeake Bay watershed. *Water Resour. Res*. Vol. 44: W09416.
- Sims, J. T., Simard, R. R., Joern, B. C., 1998. Phosphorus loss in agricultural drainage: historical perspective and current research. *Journal of Environmental Quality*. Vol. 27(2), 277–293.

- Sinclair, A., Hebb, D., Jamieson, R., Gordon, R., Benedict, K., Fuller, K., Stratton, G., et al., 2009. Growing season surface water loading of fecal indicator organisms within a rural watershed. *Water Research*. Vol. 43(5), 1199-1206.
- Smith, V. H., 1998. Cultural eutrophication of inland, estuarine, and coastal waters. Successes, limitations, and frontiers in ecosystem science. Springer-Verlag, New York, New York, USA.
- Solo-Gabriele, H. M., Wolfert, M. A., Desmarais, T. R., Palmer, C. J., 2000. Sources of *Escherichia coli* in a coastal subtropical environment. *Appl. Environ. Microbiol.* Vol. 66: 230-237.
- Steedman, R. J., 1988. Modification and assessment of an index of biotic integrity to quantify stream quality in Southern Ontario. *Can. J. Fisheries and Aquatic Sci.* Vol. 45: 492-501.
- Stein, E.D., Tiefenthaler, L.L., Schiff, K.C., 2007. Sources, patterns and mechanisms of storm water pollutant loading from watersheds and land uses of the greater Los Angeles area, California, USA. Southern California Coastal Water Research Project. Technical Report 510.
- Stumpf, C. H., Piehler, M. F., Thompson, S., Noble, R.T., 2010. Loading of fecal indicator bacteria in North Carolina tidal creek headwaters: hydrographic patterns and terrestrial runoff relationships. *Water Research*. Vol. 44, No. 16 (9): 4704-4715.
- Surbeck C.Q., Jiang, S.C., Ahn, J.H., Grant, S.B., 2006. Flow fingerprinting fecal pollution and suspended solids in stormwater runoff from an urban coastal watershed. *Environ. Sci. Technol.* Vol. 40(14): 4435-4441.
- Tiefenthaler, L.L., Stein, E. D., Schiff, K.C., 2008. Watershed and land use-based sources of trace metals in urban storm water. *Environmental Toxicology and Chemistry*. Vol. 27, No. 2: 277.
- TJCOG, 2008. Measures of the Research Triangle Region
URL:<ftp://ftp.tjcog.org/pub/tjcog/tjcogmeasures.ppt>
- USDA, 2005. "ERS/USDA Briefing Room - Land Use, Value, and Management: Major Uses of Land."
<http://www.ers.usda.gov/Briefing/LandUse/majorlandusechapter.htm>.
- US Environmental Protection Agency, 1990. Managing nonpoint source pollution: final report to Congress on section 319 of the Clean Water Act (1989). EPA/506/9-90. US EPA, Washington, DC.
- US Environmental Protection Agency, 2010. National summary of State information. URL:
http://iaspub.epa.gov.libproxy.lib.unc.edu/waters10/attains_nation_cy.control.
- Wear, D.N.; Greis, J. G., 2002. Southern forest resource assessment: summary report. Gen. Tech. Rep. SRS-54. Asheville, NC: U.S. Department of Agriculture, Forest Service, Southern Research Station. 103 p.
- Yoder, J., Roberts, V., Craun, G.F., Hill, V., Hicks, L.A., Alexander, N.T., et al. 2008. Centers for Disease Control and Prevention (CDC). Surveillance for waterborne disease and outbreaks associated with

drinking water and water not intended for drinking—United States, 2005–2006. MMWR Surveill Summ. Vol. 57(9): 39–62.